

AD _____

Award Number: DAMD17-98-1-8352

TITLE: Evaluation of the Use of DNA Adduct Dosimetry to Optimize
the Timing of High Dose Therapy for Breast Cancer

PRINCIPAL INVESTIGATOR: Richard B. Everson, M.D., Ph.D.

CONTRACTING ORGANIZATION: Wayne State University
Detroit, Michigan 48202

REPORT DATE: August 2001

TYPE OF REPORT: Annual

PREPARED FOR: U.S. Army Medical Research and Materiel Command
Fort Detrick, Maryland 21702-5012

DISTRIBUTION STATEMENT: Approved for Public Release;
Distribution Unlimited

The views, opinions and/or findings contained in this report are
those of the author(s) and should not be construed as an official
Department of the Army position, policy or decision unless so
designated by other documentation.

20020502 085

REPORT DOCUMENTATION PAGEForm Approved
OMB No. 074-0188

Public reporting burden for this collection of information is estimated to average 1 hour per response, including the time for reviewing instructions, searching existing data sources, gathering and maintaining the data needed, and completing and reviewing this collection of information. Send comments regarding this burden estimate or any other aspect of this collection of information, including suggestions for reducing this burden to Washington Headquarters Services, Directorate for Information Operations and Reports, 1215 Jefferson Davis Highway, Suite 1204, Arlington, VA 22202-4302, and to the Office of Management and Budget, Paperwork Reduction Project (0704-0188), Washington, DC 20503

1. AGENCY USE ONLY (Leave blank)		2. REPORT DATE August 2001	3. REPORT TYPE AND DATES COVERED Annual (1 Jul 00 - 1 Jul 01)	
4. TITLE AND SUBTITLE Evaluation of the Use of DNA Adduct Dosimetry to Optimize the Timing of High Dose Therapy for Breast Cancer			5. FUNDING NUMBERS DAMD17-98-1-8352	
6. AUTHOR(S) Richard B. Everson, M.D., Ph.D.				
7. PERFORMING ORGANIZATION NAME(S) AND ADDRESS(ES) Wayne State University Detroit, Michigan 48202 E-Mail: eversonr@karmanos.org			8. PERFORMING ORGANIZATION REPORT NUMBER	
9. SPONSORING / MONITORING AGENCY NAME(S) AND ADDRESS(ES) U.S. Army Medical Research and Materiel Command Fort Detrick, Maryland 21702-5012			10. SPONSORING / MONITORING AGENCY REPORT NUMBER	
11. SUPPLEMENTARY NOTES Report contains color				
12a. DISTRIBUTION / AVAILABILITY STATEMENT Approved for Public Release; Distribution Unlimited				12b. DISTRIBUTION CODE
13. ABSTRACT (Maximum 200 Words) For drugs that interact with DNA, measures of DNA damage can assess the intracellular availability of active drug at a critical molecular target. Measurements of DNA damage should reflect the integrated effect of all resistance factors, including both recognized mechanisms and uncharacterized mechanisms. Thus, molecular measures of DNA damage could provide an important tool for elucidating the time course of complex changes in resistance factors. Motivated by a recent clinical trial that demonstrated better survival when the interval between induction chemotherapy and high dose therapy was prolonged, this project is using measures of DNA damage in patient blood cells to determine whether induction chemotherapy causes transient changes in resistance. Findings indicate cyclophosphamide, cis-platin, and BCNU each produce DNA damage that can be measured in a dose dependent manner. At low doses each agent causes a similar pattern of breakage, while at high doses their pattern of damage could be distinguished. Both lymphocytes and bone marrow cells from patients can be routinely analyzed, allowing study of changes in sensitivity in multiple tissues. It is feasible to use the procedure to study whether induction therapy has a transient effect on resistance to high dose therapy.				
14. SUBJECT TERMS Breast Cancer, Transient Resistance To Chemotherapy, DNA Damage, High Dose Chemotherapy, Autologous Stem Cell Transplantation				15. NUMBER OF PAGES 59
				16. PRICE CODE
17. SECURITY CLASSIFICATION OF REPORT Unclassified	18. SECURITY CLASSIFICATION OF THIS PAGE Unclassified	19. SECURITY CLASSIFICATION OF ABSTRACT Unclassified	20. LIMITATION OF ABSTRACT Unlimited	

FOREWORD

Opinions, interpretations, conclusions and recommendations are those of the author and are not necessarily endorsed by the U.S. Army.

OK Where copyrighted material is quoted, permission has been obtained to use such material.

OK Where material from documents designated for limited distribution is quoted, permission has been obtained to use the material.

OK X Citations of commercial organizations and trade names in this report do not constitute an official Department of Army endorsement or approval of the products or services of these organizations.

N/A In conducting research using animals, the investigator(s) adhered to the "Guide for the Care and Use of Laboratory Animals," prepared by the Committee on Care and use of Laboratory Animals of the Institute of Laboratory Resources, national Research Council (NIH Publication No. 86-23, Revised 1985).

OK X For the protection of human subjects, the investigator(s) adhered to policies of applicable Federal Law 45 CFR 46.

N/A In conducting research utilizing recombinant DNA technology, the investigator(s) adhered to current guidelines promulgated by the National Institutes of Health.

N/A In the conduct of research utilizing recombinant DNA, the investigator(s) adhered to the NIH Guidelines for Research Involving Recombinant DNA Molecules.

N/A In the conduct of research involving hazardous organisms, the investigator(s) adhered to the CDC-NIH Guide for Biosafety in Microbiological and Biomedical Laboratories.

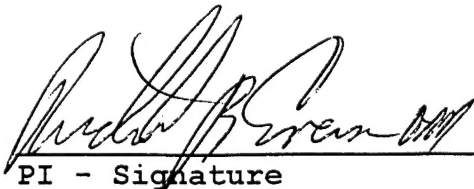
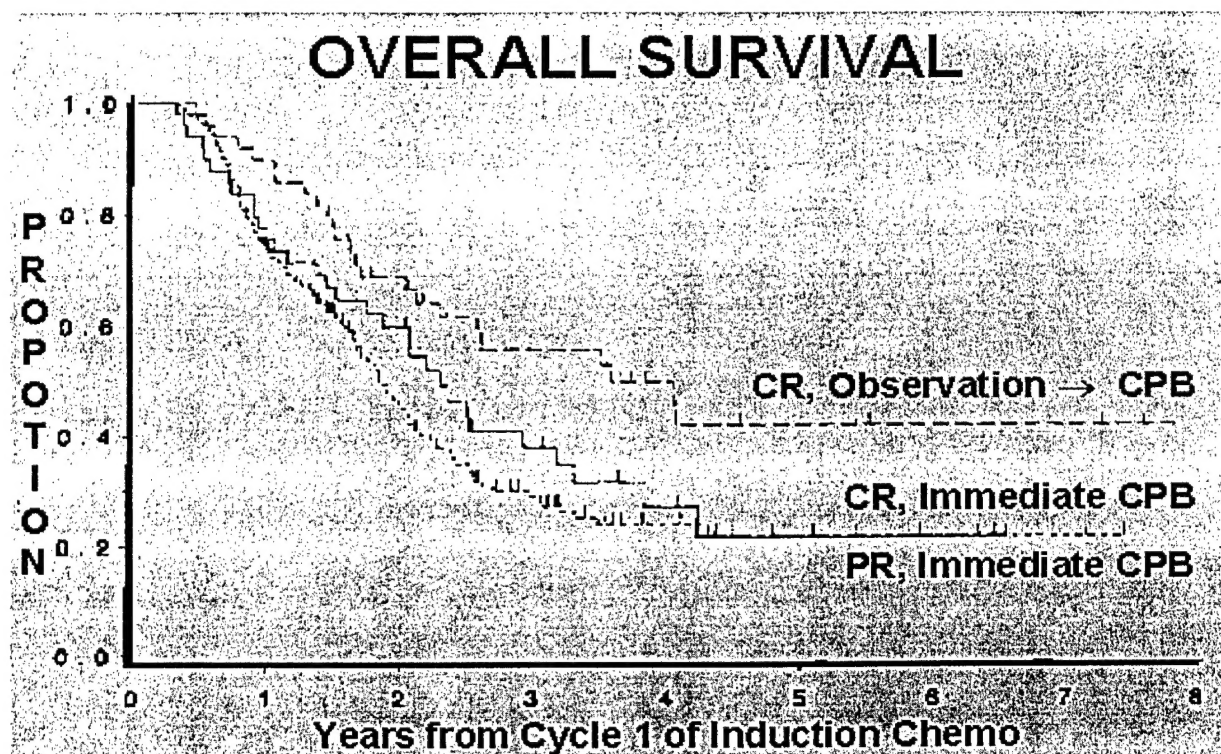
 2-28-02
PI - Signature Date

Table of Contents

Cover.....	1
SF 298.....	2
Foreword.....	3
Table of Contents.....	4
Introduction.....	5
Body.....	7-19
Key Research Accomplishments.....	20
Reportable Outcomes.....	21
Conclusions.....	22
References.....	24-25
Appendices.....	26-59

5. **Introduction** The immediate goal of this work is to contribute to understanding of the unexpected schedule dependency observed between induction and high dose therapy in a recent trial of high dose therapy with cyclophosphamide, BCNU, Cisplatin and marrow or autologous stem cell support (CPB-ACS). That trial



unexpectedly found that CPB-ACS was more successful when used at relapse (CR, Observation arm in Figure above; overall survival 40%) than immediately after induction therapy (CR, Immediate Arm in Figure above, overall survival 20%)(1). We proposed to use molecular methods to determine whether the levels of DNA damage caused by the CPB change when it is administered at different times after induction therapy. Understanding the basis for the schedule dependency of this

treatment program would directly facilitate development of more effective scheduling for this and potentially other high dose chemotherapy programs. In a broader context, work done here to develop measurements of DNA damage and molecular dose for clinical oncology will provide a rapid way to measure the effects of alternative treatment programs. These measurements would provide an approach to develop optimal treatment protocols with many fewer patients much more rapid timeframe than could be achieved using clinical outcomes.

6. Body of Report

To date our progress with respect to each of the goals of the project in the Statement of Work is as follows:

Task 1. Obtain specimens of tumor, blood cells, and other tissues from high dose chemotherapy studies for analysis. Our developmental work to improve the assays used to study induced resistance used specimens from a repository previously developed by our bone marrow transplant program. As discussed below, we have developed assays for DNA modifications that use a dramatically smaller amount of cellular material than was required for our initial pilot and developmental work. These assays measure resistance as it occurs *in vivo* by exposing the cells *in vitro*. The technical advances that allow the use of this *in vivo/in vitro* approach allowed us to study samples from the same patient obtained at different time points. This resulted in our being able to analyze specimens from the same group of patients at each time interval required for the study rather than obtain separate samples from patients in different chemotherapy arms. Thus the same patients can be used to study the effect of therapy by comparing pre treatment samples with samples obtained soon after induction therapy and at the time of recurrence, similar to Arm A, B, and C in the clinical trial described in the proposal.

Technical advances also decreased the amount of specimen needed for analyses of DNA damage. We currently require less than 2000 cells and 200 nanograms of DNA.

Taken together, the ability to use serial specimens from the same subjects will allow us to use existing specimens from studies of patients who underwent high dose

therapy to complete the work required for the study. These specimens include between 20 and 30 suitably cryopreserved specimens for each of the time intervals (induction therapy, 8 weeks after therapy prior to induction therapy, and at the time of recurrence) required for our study. We do not need patient identifiers for these studies, so that clearance for the use of the specimens is based on a protocols that qualify for exemption from IRB clearance. Use of these specimens and subjects will also allow us to directly compare DNA damage levels with the data being obtained ongoing studies of these patients, including pharmacokinetics, cellular resistance factors, and tumor vascularity that are being analyzed by other projects in our bone marrow transplantation program (as proposed for Task 5 in our statement of work).

Use of these samples, however, required that we analyze the specimens at the same time that they are being analyzed for cellular resistance factors. That in turn meant we had to delay analysis of the specimens until a fourth year of the project, when these specimens were being used. We have requested and received a one-year no-cost extension of the project, and plan to conduct all analyses required for the study using these existing specimens between April and August of 2002.

Task 2 and 3. Further develop assays for DNA adducts formed by the chemotherapeutic agents under study in order to optimize them for studying in vivo effects in patient specimen and development of in vitro approaches to studying adducts in short term primary culture.

Studies performed to date have emphasized the use of the Single Cell Gel Electrophoresis (SCGE) assay to monitor levels of DNA adducts. This assay is highly sensitive and can be performed on small numbers of cryopreserved cells. For the *in vitro* studies to be used for this

project, this technology allows analysis at multiple dose levels and replicate assays with small numbers of cells that would not be feasible with other approaches. Studies were performed with a cell line (MCF7 breast cancer cells, provided by the Tissue Culture Core of the Karmanos Cancer Institute) and peripheral blood lymphocytes and bone marrow cells from patients. Exposures to chemotherapeutic drugs was standardized at a 2 incubation hours at 37°C with various concentrations of 4-OH cyclophosphamide, cisplatin or BCNU.

The assay involves isolation of cells, embedding cells in agarose, lysing cells to remove membrane and proteins leaving DNA, denaturing DNA with high pH, electrophoresing cells, neutralizing, drying, and staining cells with a DNA stain. When performed under alkaline conditions, adducts and other alkali labile lesions are converted to breaks, such that the assay reflects levels of DNA adducts. Nucleoids with intact DNA remain circular after electrophoresis. Cells with DNA breakage reveal a brightly fluorescent circular head and a tail of damaged DNA that has electrophoreses faster than the intact DNA. These units resemble comets, hence the term "comet assay" has been applied widely to the procedure (2-4). The extent of damage is quantified by image analysis.

For most analyses the SCGE assay was performed under alkaline conditions using an adaptation of the method of Singh et al (5). To summarize the method, treated cells were suspended in 0.5% low melting point agarose in PBS at 37°C. 75 ul cell suspension was pipetted onto a frosted glass microscope slide pre-coated with 75 ul 1% normal melting point agarose and covered with a coverglass. After gelling for 5 min at 0°C, the coverglass was gently removed and a third layer of 75 ul LMP agarose was added and covered again with a coverglass. After gelling for 5 min the second time the slide was put in a tank filled with the lysis solution (2.5 M NaCl,

100 mM EDTA, 10 mM Tris, NaOH to pH 10.0 , 1% Triton X-100, and 10% DMSO) at 4°C for at least 4 hours. The slides were next placed in a horizontal electrophoresis tank containing 300 mM NaOH and 1 mM EDTA for 20 min at 4°C to allow for unwinding of the DNA prior to the electrophoresis at 25 V (1 V / cm, 300 mA) for 30 min. The slides were then washed 3 times for 5 min with cold neutralization buffer, 0.4 M Tris-HCl, pH 7.5.

Finally the slides were immersed in ethyl alcohol for 5 min before staining with Cyber Green 1. For these procedures plastics were from Corning (NY,USA) RPMI 1640 medium with phenol red and fetal bovine serum were obtained from ATCC, Manassas (VA, USA) The trypsin, salts, and buffers used in the lysis solution and the electrophoresis buffer were from Sigma, St. Louis (MO, USA).

Levels of DNA damage are determined by staining with SYBR Green and stained nucleoid were examined using a Zeiss epifluorescence microscope with 40 x Plan-neoflur objective and a 50 w mercury power source and appropriate filter. The microscope was attached to an imaging system consisting of a intensified CCD camera and a IBM compatible PC computer with a KOMET Assay Software (Kinetic Imaging, LTD). From each slide typically 50 images were analyzed sequentially; only overlapping cells were omitted from analysis. The image analysis algorithm used first applied an edge filter to define the limits of the comet, then subtracted the background (defined as the image intensity at the edge of the comet), and subsequently formed head and tail distributions for analysis. The Olive Tail moment, defined as the product of the amount of DNA in the tail multiplied by the tail length (distance between edge of comet head and end of tail), was used as a measure of the amount of damage in individual cell (6, 7). Further details of the experimental method are presented in a our standard operating procedure manual previously submitted.

We have previously shown that CPB treatment *in vivo* causes damage readily detectable by the alkaline SCGE. A limitation is that the damage appears similar for different drugs, so that *in vivo* it is likely to be difficult to discern the effects of individual drugs used for combination therapy. This problem - the relative non-specificity of the endpoint - is not a factor when studying the effects of agents *in vitro*, so we are using this approach to determining levels of DNA damage. As discussed above, this *in vivo/in vitro* approach also allows us to study the same patient at several time points. Thus each patient serves as his own control for showing timecourse effects, maximizing statistical power.

During the first and second year of the project we conducted pilot studies of several methods for analyzing DNA damage chemically. We isolated DNA by several methods, obtained adduct standards and HPLC columns suitable for chemical analysis, and procured components of instrumentation needed for chemical assays. The DNA isolation work indicated that we will obtain about 1 ug of suitable DNA per ml of blood. While this will provide sufficient material for chemical analyses *in vivo*, where a single isolation of DNA will be used for several assays, the quantities required and difficulty isolating very small amounts of DNA will preclude conducting dose-response curves with replicate analyses *in vitro* using the chemical approach. These considerations prompted focus on developing the *in vitro* SCGE assays.

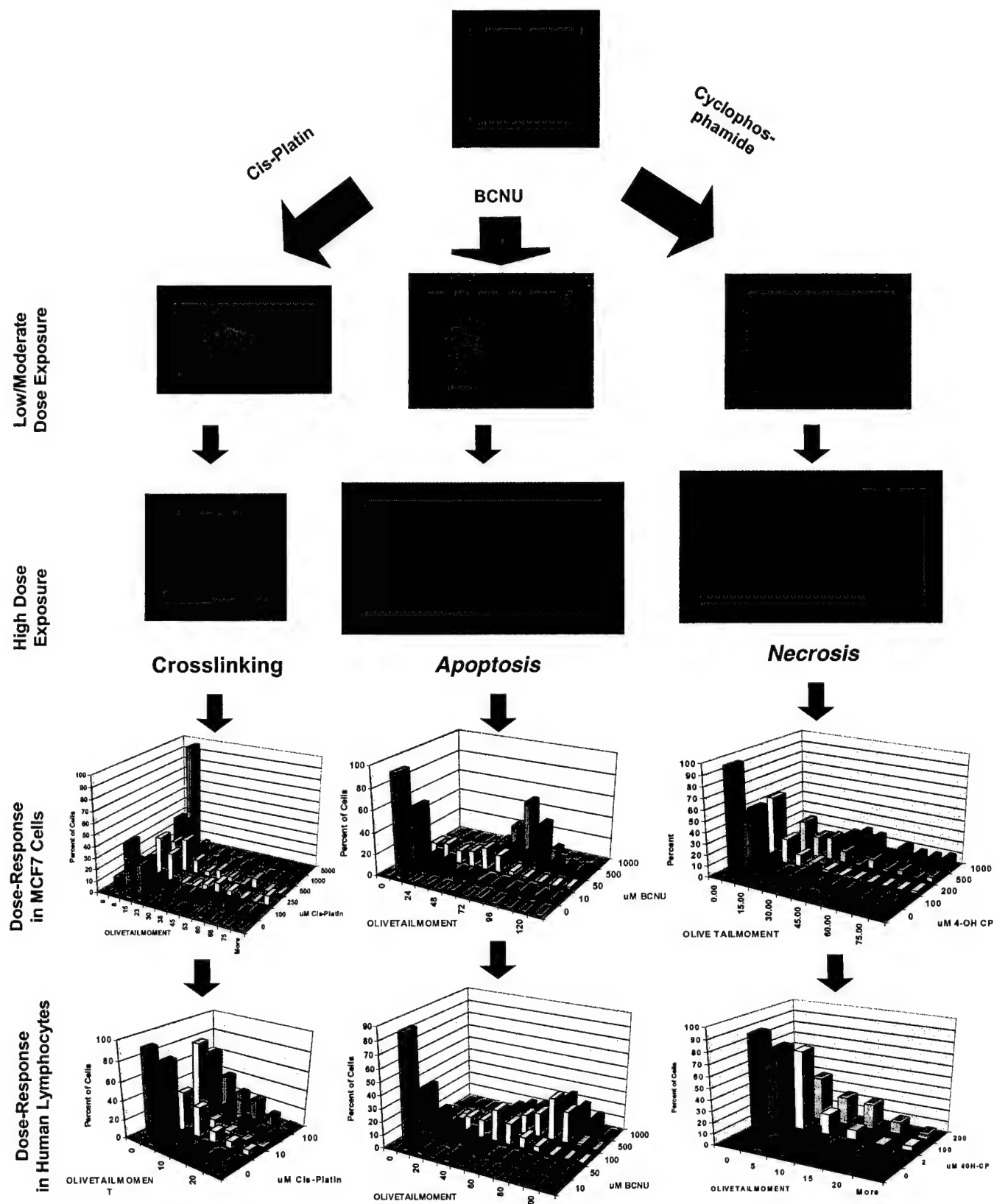
We conducted a series of *in vitro* experiments establishing dose-response relationships for DNA breakage induced by each of the individual agents used for CPB. Each agent induced DNA breakage at doses comparable to estimated AUCs that would be achievable *in vivo* with CPB therapy. Qualitatively, at low doses the pattern of breakage was grossly similar for each agent. At high doses the pattern of damage differed for each agent. These patterns were

consistent for most of the cells assayed. The patterns were also similar to those previously described in the literature for comet damage. These patterns were presented in Everson *et al.*, 2000, cited under Reportable Outcomes.

In these studies, as illustrated in the figure on the next page, damage caused by high doses of:

- Cisplatin contracted the cells, consistent with its ability to cause DNA crosslinks and patterns of Comet damage previously seen with crosslinking agents.
- BCNU caused a pattern suggesting diffusion of relatively constant molecular weight fragments prior to electrophoresis and displacement of those fragments during electrophoresis, a pattern shown to indicate apoptosis in a recent series of studies.
- 4-hydroxy cyclophosphamide (4-HC) caused broad diffusion of the DNA, a pattern previously linked with necrosis.

Quantitatively, levels of DNA damage as measured by Olive tail moment (product of DNA fluorescence in the tail and tail length) increased with increasing concentrations of each drug. Each agent caused damage in a dose-dependent manner in both MCF7 cells and primary lymphocyte cultures, with flattening at very high doses of BCNU and 4OH-CP. There was a reversal at high doses of Cisplatin consistent with its action as a crosslinker. Dose dependent



**Patterns of Damage and Dose Response Curves
for Comet Assays of Agents in CBP.**

measurements of damage can be made for a broad dose range, avoiding flattening at high doses. (Results were summarized in Everson *et al.*, 2000, cited under Reportable Outcomes).

In addition to these studies of MCF7 cell lines and primary lymphocytes, we analyzed specimens of mononuclear cells isolated by ficoll gradients of bone marrow aspirates from patients prior to CPB therapy available from our repository. These specimens were cryopreserved using a step-down freezer and stored in the vapor phase of liquid nitrogen for less than 3 months. Specimens were rapidly thawed, washed, incubated with BCNU for two hours, and analyzed by the alkali SCGE assay. Damage was readily and quantitatively detected in these cells, indicating they will allow analyses of alterations in resistance after induction therapy.

The need to analyze small numbers of cells led to further assay development. Bacso *et al.* (8), included in the Appendix, describes further developmental work with the SCGE assay which allows us to use the same cells that are analyzed for cellular damage endpoints for SCGE assays of DNA damage. For these assays cells were stained with annexin V (a marker for apoptosis) and/or propidium iodide (a marker for cell viability). Three hundred μ l of low melting point agarose was added to each 100 μ l aliquot of cells, and 80 μ l layered on the surface of slides previously prepared with a base level of agarose. After solidification, an additional agarose layer was added. The slides were read using a laser scanning cytometer (LSC) using a 488-nm argon-ion laser and collecting green fluorescence and red fluorescence emissions for measurement of the cellular endpoints. Cells could be scanned at a rate of approximately 300 per minute. After these readings the coverslips were removed and the slides were immersed in the lysis buffer described for the SCGE assay. The DNA was stained with SybrGreen, neutralized, and fixed as described above. The slides are then returned to the LSC and the same cells analyzed for

fluorescence relocated by the LSC. These cells are then analyzed by the SCGE assay by transferring the video signal from the LSC to the Komet image analysis system. This dual capability will both increase the cell numbers available for DNA damage assays by allowing the use of cells from fluorescence assays for DNA damage assays and it will allow direct comparisons of fluorescence endpoints being conducted under other studies with the DNA damage studies being conducted here.

While sample accrual to the project has continued, it has been influenced in part by recent reports concerning the effectiveness of high dose therapy, as discussed further below. This prompted a reassessment of the potential role of archived samples for the project. For example, our transplant program has accrued over 1800 specimens and colleges at Duke (where the original trial cited in the proposal was performed and the Principle Investigator of this project holds an Adjunct appointment) have several thousand additional specimens. Unfortunately the preservation methods used for these samples were not ideal for the standard SCGE assays. We have therefore expanded our emphasis on use of DNA damage assays that would be feasible with these specimens.

We assayed specimens available from a repository in which specimens were obtained and processed in a similar manner but stored at -80 deg C for over 2 years. These specimens had a very high background of damage in the pretreatment samples, levels that precluded their use for studying chemotherapy induced damage (data not shown). A variant of the SCGE assay, however, has allowed us to use the several year old cells to study both *in vivo* effects and *in vitro* changes in sensitivity to damage. This assay uses neutral conditions instead of alkali for lysis and electrophoresis: lysis is done in 30 mM EDTA, 0.5% Sodium Dodecyl Sulfate at pH 8.3, and

electrophoresis is conducted in TBE buffer (90 mM Tris base, 90 mM boric acid, 2 mM EDTA). We have determined that this assay is extremely sensitive to crosslinking. As in the standard assay, cross-linkers contract the cells, resulting in smaller tail moments. This occurred in 8 of 10 patients following CPB therapy. It also occurred in all instances following *in vitro* exposure to CisPlatin.

Chemical analyses of the addition products, which have the advantage of complete specificity for the agent being administered, are feasible in instances where larger samples of DNA are available and most desirable for discerning the effects a single agent. The high doses used clinically, fact that is the third drug given in the combination under study, and availability of a highly sensitive HPLC based assay for BCNU adducts has led to our emphasizing analysis of BCNU chemical addition products. We are using the analytic approach developed by Ye and Bordell (9) for these analyses. Methods and preliminary findings are presented in the Appendix. A continuation of this work demonstrated that it is technically feasible, but requires substantially more sample than the SGE and PCR based approaches, and tends to be less reproducible than those approaches. This has lead us not to favor continuing this analysis with the patient specimens.

While the preservation of these samples led to difficulties analyzing long sections of DNA, recent progress in polymerase chain reaction (PCR) -based approaches to adduct analysis provide a complementary approach to quantifying adducts (10-12). The methods rely on the observation that drug-DNA adducts block the progress of *taq* polymerase. Thus in the presence of DNA-adducts a repeated unidirectional PCR will accumulate multiple copies of truncated product. Alternately isolation of the specific fragments and ligation of sequence for a reverse

PCR primer allows geometric amplification of product. These methods both allow adduct detection with very small quantities of DNA. Methods for this approach are presented in reports by Grimaldi and Hartley (10, 11, 13) , and our SOP for initial steps in this work is presented in the Appendices.

We have conducted work toward making this assay approach higher throughput than that described in these reports. We have used the primers measuring DNA damage in the Human N-ras, intron 1 sequence to demonstrate the measurement of PCR product accumulation by monitoring fluorescent accumulation using the using real time polymerase chain reaction capabilities of a I-Cycler, a thermocycler with an fluorescent optical monitoring head. Analysis showed no accumulation of product until cycle 18 and then exponential accumulation of product between cycle 23 and 28. This work suggests that detection of changes in PCR could be monitored by real time fluorescent monitoring. In addition to allowing many more reactions to be run for the same effort, this approach eliminates the need to use multiple specimens in order to identify when the sample is undergoing exponential PCR required for these assays. This in turn will allow assessment with much less sample than would be required by gel-based approaches.

Task 4 and 5: Apply assays to determine the duration of the effects of induction therapy on DNA damage during high dose therapy and analyze data concerning associations between adduct levels, assays for drug pharmacokinetics, cellular resistance factors, and tumor vascularity, and use these data to develop approaches to optimize the interval between induction and high dose therapy to be tested in clinical trials. Data from initial Phase I trials of high dose chemotherapy with CPB demonstrated it had an extremely high objective response rate (about 70%), including complete responses in 17 to 37 percent of patients. Phase II trials without

induction therapy found that combining induction therapy with high dose therapy increased the complete response rate to 40 % of patients, as presented in the figure on page 6. Comparisons of the data with historical controls prompted high interest in this procedure among women with breast cancer both in and out of clinical trials (1). In 1999 and 2000, however, early results of randomized trials did not show an advantage for this approach over conventional therapy. Also, a review suggesting that one study that showed a large advantage for high dose chemotherapy was unreliable (1, 14). This prompted a marked reduction in interest in the procedure and a consequent dramatic reduction in accrual to clinical trials studying the procedure. For example, the clinical trial described in our initial proposal was designed to study 235 women in each of 3 arms for a total of 795 women. Between 1998 and 2000 less than 50 women entered the trial. While we planned including a small subset of the patients on this trial (ones on whom serial bone marrow specimens were taken for clinical purposes) for this study, low accrual made it not feasible to complete the effort here with specimens from that study. Our technical progress in reducing the sample requirements, however, has allowed us to use existing specimens obtained for other clinical studies to complete this work. Accordingly, we have confirmed the availability of specimens that will allow us to complete the studies prior the end of the current no cost extension of the project. The timing of use of these samples had to be coordinated with other uses of the samples, requiring our extending the period of the project through a no cost extension. In order to conserve resources so that they will be available to conclude this work we conducted only modest amounts of benchwork during the period covered by this report, as described above. This will ensure that adequate staffing and supplies will be available to finish the aims of the project. Given our experience during the developmental phase of the project, we plan to analyze

approximately 80 specimens obtained prior to and soon after the completion of induction chemotherapy, and at relapse. For most patients samples will be analyzed for all three time points. We plan to analyze samples by SCGE and PCR-based adduct analysis. We plan to assay a control and either one or two doses of drug for each specimen.

Although scaled down appreciable from the ancillary studies that we envisioned would be available when the project was designed, studies of transient induction of changes in drug pharmacokinetics, cellular resistance factors, and tumor vascularity are ongoing and will be available to complement our results and achieve the aim described for Task 5.

Finally, although designed around an observation and studies of high dose chemotherapy, all data obtained from this project is equally applicable to understanding resistance in conventional dose chemotherapy. We are confident it will provide useful contributions whichever treatment is the standard for care in the future.

Key Research Accomplishments

- Assays for measuring transient changes in resistance to CPB therapy following induction therapy were established using procedures that use very small numbers of cells. These have been further enhanced to allow sharing of the same cells between assays for fluorescent cellular endpoint and DNA damage. This technique will allow studies of multiple doses and replicate assays for the *in vitro* studies required for this project.
- Assays demonstrated that these procedures could be used for both lymphocytes and bone marrow cells from patients
- A modification of the SCGE assay and assays for DNA damage by biochemical and molecular methods that can be used to study transient changes in cells stored for prolonged periods
- Further assay modifications allow the same specimen to be used for cellular fluorescence and DNA damage assays, increasing capabilities and the accuracy for analyzing small number of cells.
- Additional assays for DNA modifications will allow the analysis of specimens in existing tissue repositories where sample preservation was not suitable for the SCGE approach
- Techniques for measuring DNA adducts by their interference with the polymerase chain reaction have been implemented and approaches for high-throughput analysis by real time fluorescent monitoring were developed.

7. Reportable Outcomes

Land, S.J., Bacsó, Zs., Klein, J., Eliason, J.F., and Everson R.B.

Quantitative methods for examining the drug resistance phenotype of micrometastatic cancer cells in bone marrow: DNA damage in response to in vitro drug treatment. *Proceedings of the American Association for Cancer Research* 40:403,1999

Toset, A.W., Everson, R.B.: Measurement of DNA repair in BRCA1 and BRCA2 deficient human cell lines with the Single Cell Gel Electrophoresis (SCGE) assay. *Proceedings of the American Association for Cancer Research* 41: 335, 2000

Everson, R.B., Land, S.J., Eliason, J.F., Klein, J.L., and Baynes R.D. Transient resistance to high-dose chemotherapy: Evaluation of the use of DNA-damage assays to optimize treatment schedule. *Proceedings of the Department of Defense Breast Cancer Research Program Meeting: Era of Hope* Vol. II: 690, 2000

Bacso, Z., Everson, R. B., and Eliason, J. F. The DNA of annexin V-binding apoptotic cells is highly fragmented. *Cancer Res*, 60: 4623-4628., 2000.
(While not the main report forthcoming from this project, part of my time developing methods leading to this report was supported by this grant. I apologize for leaving off support by DOD project in this report; Dr. Basco had returned to europe prior to its submission complicating communications on this.)

8. Conclusions

- Each of the agents in CPB produces DNA damage that can be measured with the SCG assays in a dose dependent manner
- At low doses all three agents cause a similar pattern of breakage, while at high doses their pattern of damage could be distinguished (Cisplatin contracted the cells, consistent with its ability to cause DNA crosslinks; BCNU caused a pattern suggesting formation of relatively constant molecular weight fragments; cylophosphamide caused fragments of diverse molecular weights.
- Both lymphocytes and bone marrow cells from patients can be routinely analyzed while sharing the specimens with other assays, allowing study of changes in sensitivity in small quantities of multiple tissues
- Analytic approaches including polymerase chain reaction and chemically based approaches that use repositories of non-ideally preserved specimens are feasible

1. Baynes, R. D., Dansey, R. D., Klein, J. L., Hamm, C., Campbell, M., Abella, E., and Peters, W. P. High-dose chemotherapy and hematopoietic stem cell transplantation for breast cancer: past or future? *Semin Oncol*, 28: 377-388., 2001.
2. Fairbairn, D. W., Olive, P. L., and KL, O. N. The comet assay: a comprehensive review. *Mutat Res*, 339: 37-59, 1995.
3. Tice, R. R. and Strauss, G. H. The single cell gel electrophoresis/comet assay: a potential tool for detecting radiation-induced DNA damage in humans. *Stem Cells (Dayt)*, 13 Suppl 1: 207-214, 1995.
4. Miyamae, Y., Zaizen, K., Ohara, K., Mine, Y., and Sasaki, Y. F. Detection of DNA lesions induced by chemical mutagens by the single cell gel electrophoresis (comet) assay. 1. Relationship between the onset of DNA damage and the characteristics of mutagens. *Mutat Res*, 393: 99-106, 1997.
5. Singh, N. P. e. a. A simple technique for quantitation of low levels of DNA damage in individual cells. *Exp. Cell Res*, 1988: 184-191, 1988.
6. Hellman, B., Vaghef, H., and Bostrom, B. The concepts of tail moment and tail inertia in the single cell gel electrophoresis assay. *Mutat Res*, 336: 123-131, 1995.
7. Olive, P. L. and Banath, J. P. Multicell spheroid response to drugs predicted with the comet assay. *Cancer Res*, 57: 5528-5533, 1997.

8. Bacso, Z., Everson, R. B., and Eliason, J. F. The DNA of annexin V-binding apoptotic cells is highly fragmented. *Cancer Res*, 60: 4623-4628., 2000.
9. Ye, Q., and Bodell, W. J. Detection of N7-(2-hydroxyethyl)guanine adducts in DNA and 9L cells treated with 1-(2-chloroethyl)-1-nitrosourea. *J Chromatogr B Biomed Sci Appl*, 694: 65-70., 1997.
10. Grimaldi, K. A., McAdam, S. R., and Hartley, J. A. PCR-based assays for strand-specific measurement of DNA damage and repair. II. Single-strand ligation-PCR. *Methods Mol Biol*, 113: 241-255, 1999.
11. Grimaldi, K. A., McAdam, S. R., Souhami, R. L., and Hartley, J. A. DNA damage by anti-cancer agents resolved at the nucleotide level of a single copy gene: evidence for a novel binding site for cisplatin in cells. *Nucleic Acids Res*, 22: 2311-2317., 1994.
12. Pfeifer, G. P., Denissenko, M. F., and Tang, M. S. PCR-based approaches to adduct analysis. *Toxicol Lett*, 102-103: 447-451., 1998.
13. Grimaldi, K. A., Bingham, J. P., and Hartley, J. A. PCR-based assays for strand-specific measurement of DNA damage and repair. I. Strand-specific quantitative PCR. *Methods Mol Biol*, 113: 227-240, 1999.
14. Antman, K. H. Overview of the six available randomized trials of high-dose chemotherapy with blood or marrow transplant in breast cancer. *J Natl Cancer Inst Monogr*, 30: 114-116, 2001.

10.

APPENDICES

	Page
Reportable Outcomes:	
Abstracts	26-28
Poster	29
Basco <i>et al.</i>	30-35
SOPs:	
DNA Isolation	36-38
DNA Precipitation	39
PCR Based Approaches to Adduct Analysis	40-44
<i>In Vitro</i> Exposures	45-49
DNA Digestion	50-56
HPLC Analysis of DNA Adducts	57-59

ABSTRACT

Quantitative methods for examining the drug resistance phenotype of micrometastatic cancer cells in bone marrow: DNA damage in response to *in vitro* drug treatment. Land, S.J., Bacsó, Zs., Klein, J., Eliason, J.F., and Everson R.B. Karmanos Cancer Inst., Wayne State University, Detroit, MI.

To examine the sensitivity of the cancer cells in patient bone marrow samples to the drugs used for high dose therapy, we have used the single cell gel electrophoresis (comet) assay for measuring DNA damage. Studies were performed with MCF7 breast cancer cells, which were incubated at 37°C with various concentrations of 4-OH cyclophosphamide, cisplatin or BCNU. Levels of DNA damage as measured by Olive tail moment (product of DNA fluorescence in the tail and tail length) increased with increasing concentrations of each drug. To determine if these measurements could be performed in the presence of human bone marrow cells, mixtures of MCF7 cells with normal marrow cells were prepared and treated with BCNU. The breast cancer cells were enriched from the mixtures using a panel of 3 murine monoclonal antibodies that recognize antigens on human breast cancer cells and magnetic beads conjugated with antibodies against the primary antibodies. The rosetted cells were enriched by magnetic sorting and analyzed using the comet assay. Only those cells associated with 3 or more beads were scored. Staining of beaded cells with antibodies against cytokeratins indicated that they were cytokeratin positive. The results for rosetted cells demonstrated similar levels of DNA damage compared to MCF7 cells assayed as a pure population. This assay has also been performed with metastatic cells isolated from patient bone marrow samples. This approach will provide a measure of drug sensitivities of malignant cells in bone marrow.

TRANSIENT RESISTANCE TO HIGH-DOSE CHEMOTHERAPY. EVALUATION OF USE OF DNA-DAMAGE ASSAYS TO OPTIMIZE TREATMENT SCHEDULE

Drs. Richard B. Everson, Susan J. Land, James F. Eliason, Jared L. Klein,
and Roy D. Baynes

Karmanos Cancer Institute and Departments of Medicine and Pathology,
Wayne State University, Detroit, MI 48201-1379.

E-mail: everson@karmanos.org

For drugs that interact with DNA, measures of DNA damage can assess the intracellular availability of active drug at a critical molecular target. Measurements of DNA damage should reflect the integrated effect of all resistance factors, including both recognized mechanisms and uncharacterized mechanisms. Thus, molecular measures of DNA damage could provide an important tool for elucidating the time course of complex changes in resistance factors.

Motivated by a recent clinical trial that demonstrated better survival when the interval between induction chemotherapy and high dose therapy was prolonged, this project is using measures of DNA damage in patient blood cells to determine whether induction chemotherapy causes transient changes in resistance. We are using the single cell gel electrophoresis (comet) assay and assays for chemical modifications to DNA. Prior to analysis of clinical specimens, studies of the capability of these methods were investigated with MCF7 breast cancer cells and human lymphocytes and bone marrow cells. The cells were incubated at 37°C with various concentrations of 4-OH cyclophosphamide, cisplatin, or BCNU.

Each agent produced DNA damage that can be measured in a dose dependent manner in the single cell gel assay. Increases were large: for example, mean levels for damage were 4.3, 10.2, and 102 with 0, 10, and 100 μ M BCNU, respectively. At low doses, each agent causes a similar pattern of breakage, while at high doses their pattern of damage could be distinguished. Cisplatin contracted the cells, consistent with its ability to cause DNA crosslinks. BCNU caused a pattern suggesting diffusion of relatively constant molecular weight fragments prior to electrophoresis and displacement of those fragments during electrophoresis, a pattern shown to indicate apoptosis. 4-OH cyclophosphamide caused broad diffusion of the DNA, a pattern previously linked with necrosis.

Both lymphocytes and bone marrow cells from patients can be routinely analyzed, allowing study of changes in sensitivity in multiple tissues. It is feasible to use the procedure to study whether induction therapy has a transient effect on resistance to high dose therapy; these studies are underway.

The U.S. Army Medical Research and Materiel Command under DAMD17-98-1-8352 supported this work.

Measurement of DNA repair in BRCA1 and BRCA2 deficient human cell lines

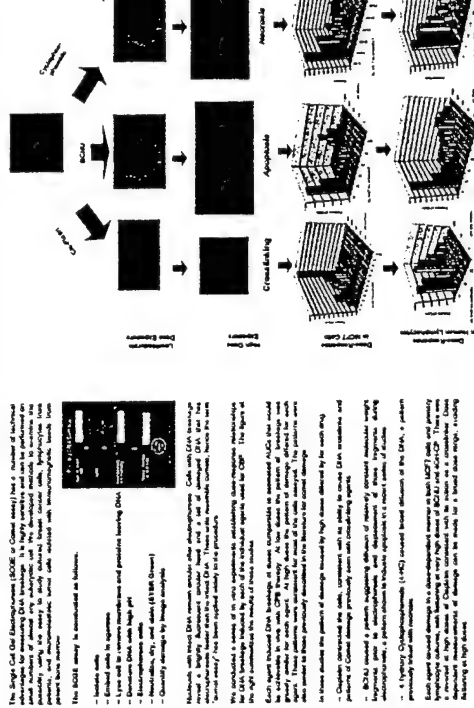
with the single cell gel electrophoresis (SCGE) assay

Toset, A.W. and Everson R.B., Karmanos Cancer Inst., Wayne State University, Detroit, MI

Recent investigations link the function of BRCA1 and BRCA2 with deficiencies in DNA repair, including repair of oxidative damage, radiation damage, and damage from chemotherapeutic agents that cause double strand breaks. Because of its ability to analyze small numbers of cells from biopsy samples, use of the SCGE to measure these deficiencies would facilitate translational research by allowing parallel studies of cell lines and other experimental systems and clinical specimens. To ascertain the effectiveness of the SCGE assay for characterizing diminished DNA repair in this setting, we determined the ability of human cancer cell lines harboring mutations in BRCA1 (breast line HCC1937 containing a homozygous deletion and lymphoblastoid line HCC1937L containing a heterozygous deletion) and BRCA2 (pancreatic line Capan-1 containing a homozygous deletion) to repair DNA damage caused by treatment with radiation, etoposide, and hydrogen peroxide. The breast cancer cell line MCF7 and pancreatic cancer cell line BxPC-3 were used as controls. DNA damage was induced in these cell lines by irradiation on ice, 5 minute exposure to hydrogen peroxide, or 1 hour exposure to etoposide. Cells were allowed to repair for 1 hour at 37 deg C and damage measured by the alkaline SCGE. Except for the highest dose of irradiation (10,000 R), where repair was less than 30% for both the MCF7 and HCC1937 lines, repair was proficient for each agent, dose, and cell line. Most cell lines repaired over 90 percent of damage from H₂O₂, 80 percent of damage from etoposide, and 60 percent of damage from 3,000R, with no consistent differences between BRCA mutant and control lines. Human BRCA deficient cell lines showed proficient repair as measured by the alkaline SCGE assay.

Transient Resistance To High-dose Chemotherapy: Evaluation Of The Use Of DNA-damage Assays To Optimize Treatment Schedule Richard B. Everson, Susan J. Land, James F. Eliason, Jared L. Klein, and Roy D. Baynes Karmanos Cancer Institute and Departments of Medicine and Pathology, Wayne State University, Detroit, MI 48201-1379

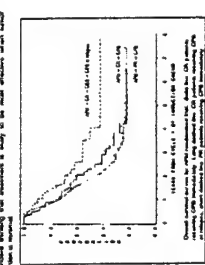
Methods and Results: SCGE/Comet Assays of MCF7 Cells and Human Lymphocytes



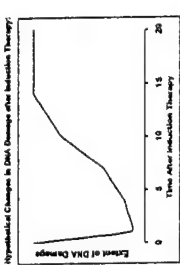
Patterns of Damage and Comet Tail Length Curves for Cisplatin and Doxorubicin

Results of the AFM Randomized Trial

The AFM Randomized Trial compared the induction therapy with cisplatin, 5-FU, and doxorubicin (CDDP) to the induction therapy with cisplatin, 5-FU, and doxorubicin (CDDP) plus granulocyte colony-stimulating factor (G-CSF). The results of the trial are shown in the following table:



On the basis of the results of the AFM Randomized Trial, the induction therapy with cisplatin, 5-FU, and doxorubicin (CDDP) plus granulocyte colony-stimulating factor (G-CSF) was found to be superior to the induction therapy with cisplatin, 5-FU, and doxorubicin (CDDP) alone. The results of the trial are shown in the following table:



The AFM Randomized Trial compared the induction therapy with cisplatin, 5-FU, and doxorubicin (CDDP) to the induction therapy with cisplatin, 5-FU, and doxorubicin (CDDP) plus granulocyte colony-stimulating factor (G-CSF). The results of the trial are shown in the following table:

The AFM Randomized Trial compared the induction therapy with cisplatin, 5-FU, and doxorubicin (CDDP) to the induction therapy with cisplatin, 5-FU, and doxorubicin (CDDP) plus granulocyte colony-stimulating factor (G-CSF). The results of the trial are shown in the following table:



The AFM Randomized Trial Design

ABSTRACT

The AFM Randomized Trial compared the induction therapy with cisplatin, 5-FU, and doxorubicin (CDDP) to the induction therapy with cisplatin, 5-FU, and doxorubicin (CDDP) plus granulocyte colony-stimulating factor (G-CSF). The results of the trial are shown in the following table:

The AFM Randomized Trial compared the induction therapy with cisplatin, 5-FU, and doxorubicin (CDDP) to the induction therapy with cisplatin, 5-FU, and doxorubicin (CDDP) plus granulocyte colony-stimulating factor (G-CSF). The results of the trial are shown in the following table:

Each of the agents in CDDP produces DNA damage that can be measured with the SCGE assay in a dose dependent manner.

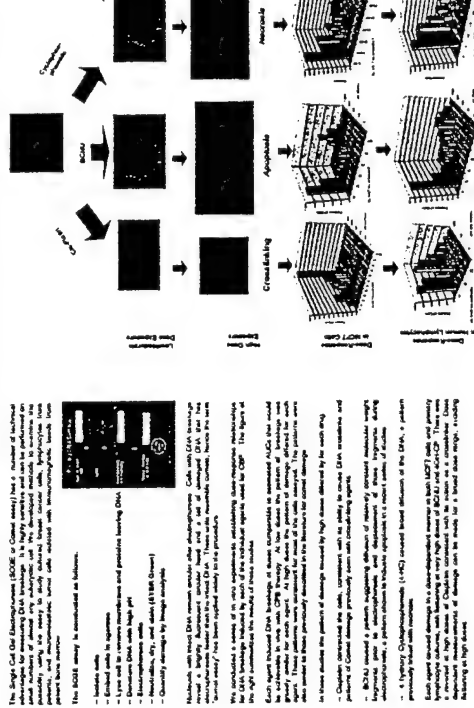
At low doses all three agents cause a similar pattern of breakage, while at high doses their pattern of damage could be distinguished.

Both lymphocytes and bone marrow cells from patients can be routinely analyzed, allowing study of changes in sensitivity in multiple tissues.

It is feasible to use the procedure to study whether induction therapy has a transient effect on resistance to high dose therapy.

Specimen collection is ongoing to use this approach to study transient resistance to chemotherapy.

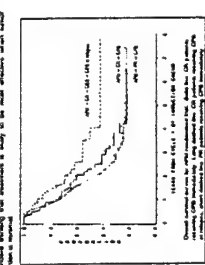
Methods and Results: SCGE/Comet Assays of MCF7 Cells and Human Lymphocytes



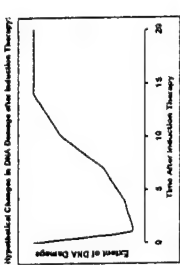
Patterns of Damage and Comet Tail Length Curves for Cisplatin and Doxorubicin

Results of the AFM Randomized Trial

The AFM Randomized Trial compared the induction therapy with cisplatin, 5-FU, and doxorubicin (CDDP) to the induction therapy with cisplatin, 5-FU, and doxorubicin (CDDP) plus granulocyte colony-stimulating factor (G-CSF). The results of the trial are shown in the following table:



On the basis of the results of the AFM Randomized Trial, the induction therapy with cisplatin, 5-FU, and doxorubicin (CDDP) plus granulocyte colony-stimulating factor (G-CSF) was found to be superior to the induction therapy with cisplatin, 5-FU, and doxorubicin (CDDP) alone. The results of the trial are shown in the following table:



ABSTRACT

The AFM Randomized Trial compared the induction therapy with cisplatin, 5-FU, and doxorubicin (CDDP) to the induction therapy with cisplatin, 5-FU, and doxorubicin (CDDP) plus granulocyte colony-stimulating factor (G-CSF). The results of the trial are shown in the following table:

The AFM Randomized Trial compared the induction therapy with cisplatin, 5-FU, and doxorubicin (CDDP) to the induction therapy with cisplatin, 5-FU, and doxorubicin (CDDP) plus granulocyte colony-stimulating factor (G-CSF). The results of the trial are shown in the following table:

The AFM Randomized Trial Design

The U.S. Army Medical Research and Materiel Command under DAMD17-96-1-4352 partially supported this work.

The DNA of Annexin V-binding Apoptotic Cells Is Highly Fragmented¹

Zsolt Bacsó,² Richard B. Everson, and James F. Eliason³

Barbara Ann Karmanos Cancer Institute, Wayne State School of Medicine Detroit, Michigan 48201

ABSTRACT

Jurkat leukemia cells induced to undergo apoptosis by treatment with an antibody against the Fas receptor have two annexin V (AV)-binding subpopulations: (a) single-positive cells that bind AV but not propidium iodide (PI); and (b) double-positive cells that bind AV and PI. The single-positive population is thought to represent an early stage of apoptosis. We have examined the relationship between AV binding and a classical characteristic of apoptosis, DNA fragmentation. Time course studies with Jurkat cells treated for 1, 2, or 4 h with anti-Fas indicated that the proportion of AV-binding cells was increased after 2 h. A significant increase in DNA fragmentation was observed only at 4 h as measured by the mean tail moment determined with the alkaline single cell gel electrophoresis (comet) assay. This correlation suggests a temporal relationship between the two parameters, but does not provide direct evidence of what happens in individual cells. We developed a method to measure fluorescent markers of cellular structure or function with a laser scanning cytometer and then perform the comet assay on the same cells. Cells in each AV-binding subpopulation were re-examined before and after electrophoresis. Most AV⁺/PI⁻ cells had no DNA damage, although a few cells showed a pattern of damage characteristic for apoptosis. Double-positive cells all had damaged DNA; approximately half had the apoptotic pattern, and the rest had a pattern typical for necrosis. Nearly all of the single-positive cells had damaged DNA with the apoptotic pattern. Both AV⁺ populations contained cells with little or no detectable DNA after electrophoresis, indicating that the DNA was highly fragmented. These results indicate that AV binding is an excellent marker for apoptotic cells, but that these cells already have fragmented DNA.

INTRODUCTION

Programmed cell death (apoptosis) is an important process in normal development and in tissue homeostasis, as well as a key mechanism by which anticancer therapies exert their cytotoxic effects. Agents like anticancer drugs and ionizing radiation that damage DNA induce apoptosis through a p53-dependent pathway (1). Binding of p53 and other nuclear proteins to the sites of damage in the DNA appears to trigger the apoptotic process. Another mechanism that can induce apoptosis involves the interaction of proteins such as Fas (CD95) or tumor necrosis factor with their receptors on the surface of cells. Signaling from these so-called death receptors starts the apoptotic process (2).

Regardless of how the apoptotic process has been initiated, by intrinsic signals or extrinsic signals involving death receptors, a hallmark of apoptosis is fragmentation of the DNA. Two main steps have been identified for apoptotic DNA fragmentation (3). The first involves formation of high molecular size DNA fragments of 50–300 kb. This process is widely observed in different cells and is propagated through single- and double-strand breaks in the DNA. The second step generates small, 200–300-bp DNA fragments. These

small fragments lead to DNA ladder formation classically associated with apoptosis, although it can be absent in some cell types (4).

Another characteristic of cells undergoing apoptosis is the capacity to bind the protein AV.⁴ AV binds to PS, which is normally located on the inner leaflet of the plasma membrane, but it is externalized to the outer leaflet during apoptosis. PI staining is widely used to discriminate living cells, which exclude this DNA dye, from dead cells, which are permeable to it. In populations of cells undergoing apoptosis, there are some cells that bind AV but are not stained with PI. This "single-positive" population is thought to represent cells in an early stage of apoptosis because the cells apparently exclude PI and because it appears earlier than DNA ladders can be seen (5).

The Fas-induced apoptotic pathway in Jurkat cells is one of the best-examined models of apoptosis. As in other apoptotic pathways, the activation of cysteine-dependent aspartate-directed proteases, *i.e.*, caspases, is crucial (2). The initial events may be reversible, but in turn, initiate irreversible processes belonging to the "execution phase," such as externalization of phosphatidylserine in the plasma membrane and fragmentation of nuclear DNA.

DNA fragmentation related to apoptosis is usually measured using mass biochemical methods. With heterogeneous cell populations, these techniques will miss contributions from small subpopulations. The comet assay, on the other hand, measures DNA fragmentation on a single cell level, allowing analysis of subpopulations of cells. Our immediate aim was to develop a method to measure the relationship between nuclear DNA fragmentation and membrane PS externalization, two hallmarks of apoptotic cell death on a cell-by-cell basis. We show that there is a high degree of DNA fragmentation in Jurkat cells that stain with AV after apoptosis is induced by treatment with an antibody against Fas.

MATERIALS AND METHODS

Cell Culture. Jurkat T lymphocytic leukemia cells (American Type Culture Collection, Manassas, VA) were kept in continuous logarithmic growth by passaging them at a concentration of 2.5×10^5 cells/ml every other day in RPMI 1640 medium supplemented with 10% fetal bovine serum (Life Technologies, Inc., Grand Island, NY), 10 mM HEPES (Sigma, St. Louis, MO), and 50 µg/ml gentamicin (Life Technologies, Inc.).

Induction of Apoptosis. Cells were subcultured 1 day before each experiment was performed. Apoptosis was induced by transfer into fresh culture medium containing 2 µg/ml of a monoclonal antibody against human Fas (CD95; mouse IgG1, clone DX2.1; R&D Systems, Minneapolis, MN) and 2 µg/ml of protein G (Sigma). The cells were incubated at 37°C for various periods of time. In some experiments, control cells were incubated with protein G alone.

AV and PI Staining. After incubation with anti-Fas and/or protein G, cells were harvested by centrifugation for 5 min at $200 \times g$ and were resuspended in AB buffer (140 mM NaCl and 2.5 mM CaCl₂). Aliquots containing 1×10^5 cells in 100 µl of buffer were stained with 10 µl of PI (50 µg/ml) solution and with 5 µl of FITC-conjugated AV (17.6 µg/ml; PharMingen, San Diego, CA) for 5 min at 37°C. After staining, 400 µl of AB buffer were added to the cells, and samples were stored on ice until data acquisition. Measurements were completed within 1 h.

Flow Cytometry. Flow cytometric analysis was performed using a FAC-Scan flow cytometer (Becton Dickinson, San Jose, CA). Photomultiplier

Received 2/22/00; accepted 6/19/00.

The costs of publication of this article were defrayed in part by the payment of page charges. This article must therefore be hereby marked *advertisement* in accordance with 18 U.S.C. Section 1734 solely to indicate this fact.

¹ Supported in part by a Virtual Discovery Grant from the Karmanos Cancer Institute.

² Present address: Department of Biophysics and Cell Biology, Faculty of Medicine, University of Debrecen, Debrecen, Hungary H-4012. E-mail: bacszo@jaguar.dote.hu.

³ To whom requests for reprints should be addressed, at Barbara Ann Karmanos Cancer Institute, HWCRC 724, Detroit, MI 48201. Phone: (313) 966-7858; Fax: (313) 966-7558; E-mail: eliasonj@karmanos.org.

⁴ The abbreviations used are: AV, annexin V; PI, propidium iodide; PS, phosphatidylserine; LMP, low melting point; LSC, laser scanning cytometer.

voltages were adjusted to have the unlabeled Jurkat cell population fall in the first decade of fluorescence. Cells labeled with only AV-FITC or PI were used to adjust the compensation. Data acquisition and analysis were performed by the CellQuest program (Becton Dickinson).

Single Cell Gel Electrophoresis (Comet Assay). Agarose-coated slides were made by dipping half-frosted slides (Superfrost+, VWR, Batavia, IL) into hot (80°C) 1% agarose (SIGMA) in distilled water and drying in air. A total of 2×10^4 cells were suspended in 80 μ l of 0.75% LMP agarose (Boehringer Mannheim, Indianapolis, IN) prepared in AB buffer and layered onto the agarose-coated slides. The agarose was solidified by placing the slides on ice for 2 min. A second layer of 0.75% LMP agarose was applied to cover the cells. The cells were lysed in ice-cold alkaline lysis buffer [1% laurylsarcosine, 2.5 M NaCl, 10 mM Tris, 100 mM EDTA, 10% DMSO, 1% Triton-X-100 (pH 10)] for 1 h. Then DNA was unwound for 15 min in cold running buffer (300 mM NaOH, 1 mM EDTA) and electrophoresed for 20 min. Slides were neutralized in cold 0.4 M Tris buffer (pH 7.4) for 5 min and fixed in cold ethanol for 5 min. The slides were stained with SYBR Green I (Molecular Probes, Eugene, OR) diluted 1:1000 in TE [10 mM Tris (pH 8.0) and 2 mM EDTA] for 15 min and covered with antifade solution (ProLong, Molecular Probes). Comets were quantitatively evaluated using a fluorescence microscope (Zeiss, Germany) with the Komet 3.1 image analysis system (Kinetic Imaging, Bromborough, United Kingdom). LMP agarose was prepared in AB buffer.

Tail moment is defined as a product of the distance between the head and tail mass centers and the relative amount of DNA in the tail compared with the total DNA in each comet (6).

Combination Assay Using the LSC. Cells were stained with AV and PI as described above. To each 100- μ l aliquot of labeled cells, 300 μ l of 1% LMP agarose were added. From this mixture, 80 μ l were layered on the surface of each agarose-coated slide. After the agarose with cells solidified, a second layer of agarose was added, and coverslips were placed on top. The slides were kept on ice until measurements were done using the LSC (CompuCyt Corporation, Cambridge, MA). The hardware was controlled by the WinCyt 3.1 software for Windows NT. The 488-nm argon-ion laser line was used for excitation. Green fluorescence and red fluorescence emission as well as forward scatter light was collected. The contour threshold was setup using the "added" parameter, which is a sum of the forward scatter light, green fluorescence, and red fluorescence parameters. Compensation was determined using single-labeled samples. We have used a 10 \times objective to reduce the time needed for scanning a given area. The size of an apoptotic comet is in the range of 100 μ m, which determines maximal cell concentration that can be used. Under our experimental conditions, 3000 cells on each slide could be scanned in \sim 10 min. After the AV-PI measurements were completed, coverslips were removed from the slides, and they were immersed in the lysis buffer. The DNA was stained with SYBR Green I, neutralized, and fixed as described above. To perform the comet assay, the cells of interest were relocated by the LSC based on the previous measurements. The video signal from the color video camera of the LSC was ported over to the Komet 3.1 image system.

RESULTS

The LSC provides quantitative fluorescence data similar to that obtained by flow cytometry. With Jurkat cells treated with anti-Fas and stained with AV-FITC and PI, both methods identify three distinct populations (e.g., see Fig. 3A): double-negative cells (AV⁻/PI⁻), single-positive cells (AV⁺/PI⁻), and double-positive cells (AV⁺/PI⁺). Fig. 1A summarizes the results of several experiments examining the time course of appearance of AV⁺ single-positive cells after treatment with anti-Fas. Both cytometric measurements show a similar pattern, although at each time point, the LSC detects more AV⁺ cells than does the flow cytometer. Because the LSC is a microscope-based measurement and the cells remain attached to the slide, each event can be re-examined and each could be confirmed to be a cell (see Fig. 3). One h after induction, there was only a small increase in the percentage of single-positive cells, but by the second hour, \sim 15% of the cells measured were positive by the LSC and 5% by flow cytometry.

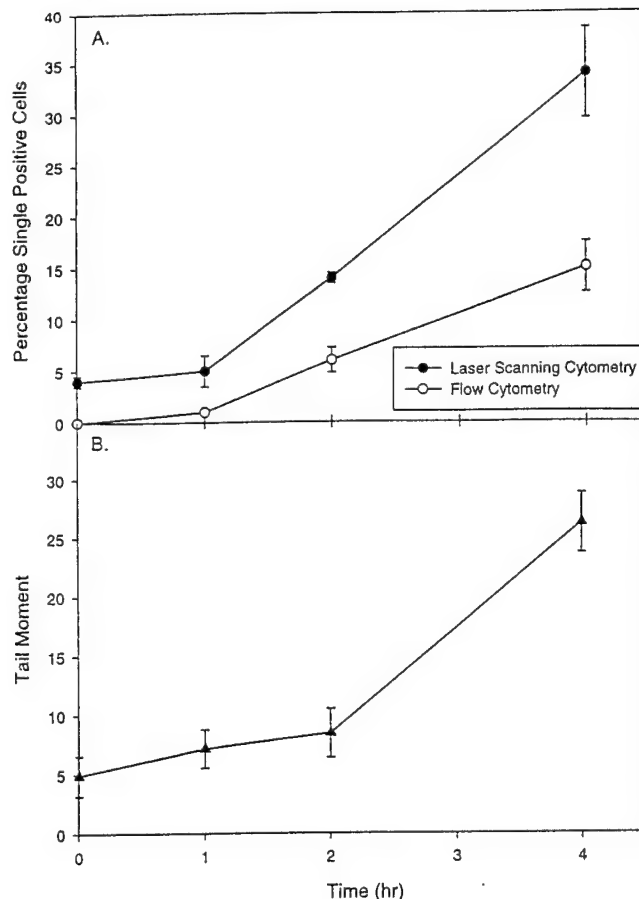


Fig. 1. Time course of induced apoptosis in Jurkat cells measured by flow cytometry, laser scanning cytometry, or the comet assay. A, \circ , mean percentage of AV⁺/PI⁻ cells from three independent experiments using the flow cytometer. \bullet , mean percentage of AV single-positive cells from 12 (0 h), 6 (1 h), 8 (2 h), or 4 (4 h) independent experiments using the LSC. B, \blacktriangle , mean tail moments measured for 100 cells each from five independent experiments. Vertical bars, \pm 1 SE.

The kinetics of apoptosis in these cells were also examined using the standard comet assay. After electrophoresis and staining, 100 cells were randomly selected and scored for DNA damage as measured by the tail moment. The results (Fig. 1B) indicate a slow increase in the mean tail moment during the first 2 h, with a large increase by 4 h after induction. More detailed results for the 0- and 2-h time points for a typical experiment are shown in Fig. 2. The histograms for tail moments are depicted in Fig. 2, A and B. The relationships between tail moments and total DNA staining are shown in Fig. 2, C and D. The tail moments for control cells were very low, with most being \leq 10 (Fig. 2A). After 2 h of treatment with anti-Fas, some tail moments were considerably $>$ 40.

The time course studies depicted in Fig. 1 suggest that the increase in tail moments of the anti-Fas-treated cells may occur somewhat later than the increase in AV binding. However, this approach does not provide information as to how much DNA fragmentation is present in each AV⁺ cell. To examine this more precisely, analyses were performed using the LSC. Cells in each area of interest of the scattergrams were relocated. Representative bright field and epifluorescence photomicrographs were taken of these cells. They were then lysed and electrophoresed for the comet assay. The locations of the cells of interest were re-examined to determine the extent of DNA fragmentation.

The results of a representative experiment are shown in Fig. 3. The bright field photograph of a typical double-negative cell shows a

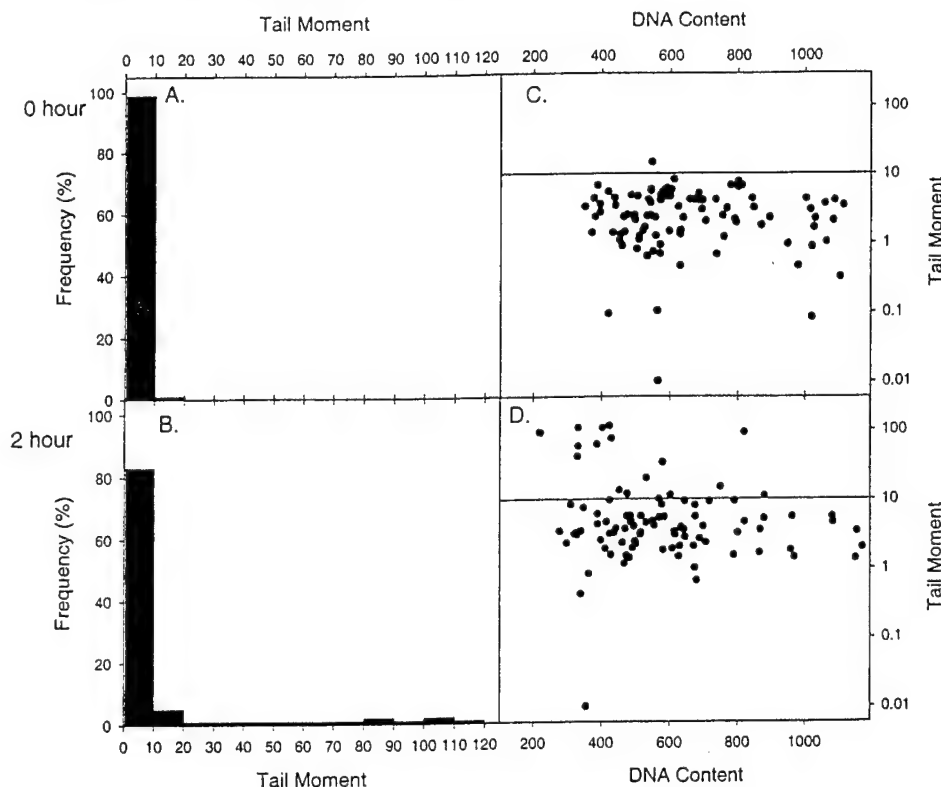


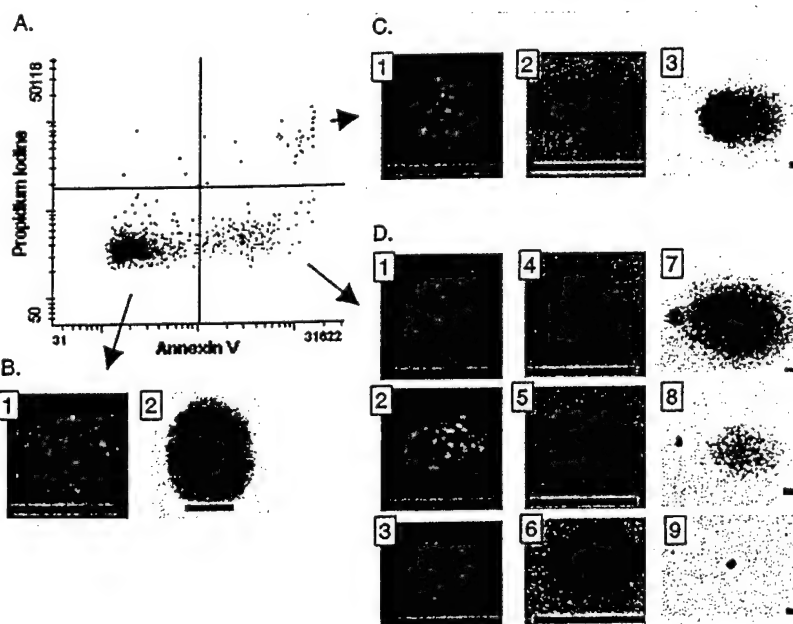
Fig. 2. Distribution of tail moments (A and B) and relationships to DNA content (C and D) in Jurkat cells without (A and C) and with (B and D) anti-Fas for 2 h. The results for a representative experiment from a series of seven are depicted.

round cell with a sharply defined cell membrane (Fig. 3B1). After electrophoresis, the nuclei of most cells in this population remained as bright circles (Fig. 3B2). The cells in the double-positive population had indistinct borders when viewed under a bright field (Fig. 3C1). AV staining on these cells was usually uniform as shown in Fig. 3C2. Many of the cells in this population gave a typical "comet" pattern for their DNA after electrophoresis (Fig. 3C3) with a bright "head" where the nucleus was and a tail of damaged DNA. This pattern is characteristic of necrotic cells. The single-positive cells had some definition around them, but their shapes were much more irregular than those of the double-negative population (Fig. 3, D1-3) and often showed

localized staining with AV around the edges (Fig. 3, D4-6). The DNA patterns are typical of apoptotic cells (Fig. 3, D6-9), forming clouds of small pieces of DNA that migrate away from the original site, some with only traces of DNA staining (Fig. 3D8).

Based on analysis of a number of experiments, the DNA patterns of PI/AV-stained cells could be placed in four basic categories: (a) normal nuclei without DNA damage having all DNA remaining at the site of the nucleus (Fig. 3B2); (b) "Comet" with considerable DNA both in the head and in the tail, characteristic of necrotic DNA damage (Fig. 3C3); (c) "Apoptotic comets" with little DNA in the head, usually as a ring with less DNA in the center of the head, followed by

Fig. 3. Typical bright field and fluorescence images of Jurkat cells treated for 2 h with anti-Fas in different AV-FITC- and PI-staining subpopulations. After staining, the cells were embedded in agarose on a slide, and fluorescence was measured using the LSC. Events were relocated, and images were made for each subpopulation identified in the scatter plot (A). Bright field images of cells (B1, C1, D1, D2, and D3) as well as AV fluorescence images (C2, D4, D5, and D6) were recorded before lysis and electrophoresis, after which SYBR Green I fluorescence images were recorded (B2, C3, D7, D8, and D9). The characteristic DNA staining patterns after conducting the comet assay are the following: normal DNA (B2), "necrotic" comet (C3), "apoptotic" comet with measurable DNA (D7), "apoptotic remnant" with trace DNA in its tail (D8), and "apoptotic remnant" without DNA (D9). Each row shows a set of images obtained sequentially from the same cell. Bars, 10 μ m. As can be seen, the images of the comets were taken with a lower magnification, and the stage was moved to center the comet because the LSC centers on the original location of the cells, where the apoptotic remnants are found.



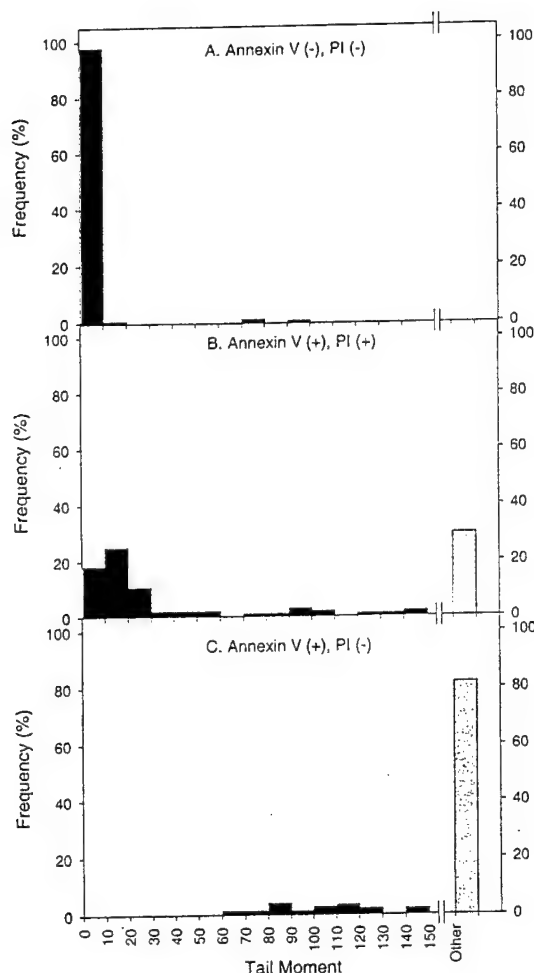


Fig. 4. Distributions of tail moments in AV⁻/PI⁻ (A), AV⁺/PI⁺ (B), and AV⁺/PI⁻ (C) Jurkat cells after treatment with anti-Fas for 2 h. "Other" consists of "apoptotic remnants" and those "apoptotic" comets where it was not possible to measure tail moments because there was little or no DNA remaining at the cellular locations after electrophoresis. The results are for a representative experiment from a series of six.

a large cloud. This is characteristic of apoptotic DNA fragmentation (Fig. 3D7). In certain cases, at the sites of nuclei, only traces of DNA remained, appearing as ring-shaped objects (not shown). Classification of these based on the relocalization of a large number of cells and the presence of DNA clouds with various fluorescent intensities indicates that they represent a continuum with progressively less DNA; and (d) Small condensed particles at the original locations of the nuclei with small amounts of fragmented DNA in a cloud (see left side of Fig. 3D8) or even without a DNA tail (Fig. 3D9). The color of these condensed particles on SYBR Green I-stained slides was more yellow than the stained DNA. Because SYBR Green I can also stain hydrophobic proteins, this may be an indication that they were not composed of pure DNA. We will refer to these as "apoptotic remnants."

These patterns are segregated between the different subpopulations

in the AV-PI scattergrams. Table 1 shows the proportions of each in these populations of cells treated with anti-Fas for 2 h and control cells. The double-negative population primarily consisted of cells with unfragmented DNA. In both treatment groups, >90% of the cells in this population had intact DNA. The AV single-positive population in either treatment group demonstrated highly fragmented apoptotic DNA and apoptotic remnants, with no cells having a necrotic pattern and only a few with undamaged DNA. In the double-positive population, there were both necrotic and apoptotic comets. Although treatment changes the numbers of cells in the single- and double-positive subpopulations compared with untreated cells, the type of damage in each subpopulation is the same.

We have measured the tail moments associated with each subpopulation of cells by transferring the signal from the video camera on the LSC to the image analysis system for the comet assay. Many apoptotic events in the single-positive and double-positive populations could not be scored because the total amount of DNA was too low for accurate image analysis. This includes some of the apoptotic comets that had lost most of their DNA as well as the apoptotic remnants. These were counted manually and would not have been identified in the standard alkaline comet assay. The results are shown in Fig. 4 and Table 1. The double-negative population had unfragmented nuclei, with 96.6% of the cells having tail moments <10 (Fig. 4A). After anti-Fas treatment, the proportion of cells with normal nuclei dropped to 90.8%, and those with apoptotic patterns increased from 3.0 to 8.6% (Table 1). In the double-positive population, there was a wide range of values with necrotic comets having tail moments between 10 and 40 and apoptotic comets with tail moments >40 (Fig. 4B; Table 1). This population also contained apoptotic remnants. Most of the events in the single-positive populations could not be measured, and those that could had tail moments >60 (Fig. 4C). All represented apoptotic patterns. In cells treated with anti-Fas, there was a shift to earlier stages of apoptosis, with apoptotic comets increasing from 35 to 85% and apoptotic remnants decreasing from 58 to 12% of the population. Thus, as cells are induced into apoptosis, earlier stages predominate (Table 1).

The relative proportions of measurable apoptotic comets to late apoptotic events, such as apoptotic remnants that could not be characterized by tail moment measurements in the single-positive population of cells treated with anti-Fas, were calculated. After untreated cells have been harvested and prepared for measurement (0 h), ~5% are single positive (Fig. 1), and 85% of these do not have sufficient DNA to measure comet tail moments. As the number of single positive cells increases after the addition of anti-Fas, the proportion of measurable comets increases progressively from 15 to 22%, and then to 29%, after 1 and 2 h. By the third hour of treatment, 38% of the comets represent these early stages as new cells are induced to undergo apoptosis. This proportion falls rapidly again to 12% in the next hour.

Similar studies were performed with MCF-7 breast cancer cells that had been serum-starved to induce apoptosis and with PC3 prostate cancer cells treated with ionizing radiation. The results showed that the AV single- and double-positive populations had similar DNA

Table 1 Pattern of DNA damage in cells labeled with AV and PI after 2-h treatment with anti-Fas^a

Pattern: Anti-Fas:	Normal DNA (%)		Necrotic comet (%)		Apoptotic comet (%)		Apoptotic remnant (%)	
	-	+	-	+	-	+	-	+
AV ⁻ /PI ⁻	96.6 ± 1.1	90.8 ± 3.2	0.4 ± 0.4	0.6 ± 0.4	2.2 ± 0.8	7.2 ± 2.2	0.8 ± 0.6	1.4 ± 1.2
AV ⁺ /PI ⁻	6.5 ± 1.2	2.4 ± 1.3	0 ± 0	0 ± 0	35.0 ± 2.0	85.3 ± 5.8	58.5 ± 4.7	12.3 ± 4.5
AV ⁺ /PI ⁺	0 ± 0	0 ± 0	56.2 ± 5.5	45.1 ± 1.4	23.9 ± 1.5	38.7 ± 2.5	19.9 ± 1.1	16.2 ± 0.7

^a Results represent averages from four experiments ± 1 SE. At least 100 cells were counted in each experiment for each AV, PI subpopulation, when possible. Data are expressed as percentages.

patterns to those of Jurkat cells induced with anti-Fas. Single-positive cells were all apoptotic, with a high degree of fragmentation and DNA loss appearing the same as those in Fig. 3D. Double-positive cells, on the other hand, had a mixture of apoptotic and necrotic comets similar to those in Fig. 3C.

DISCUSSION

The process of apoptosis has received a great deal of attention in experimental oncology. Defects in this pathway early during carcinogenesis can ultimately lead to cancer formation (7) and later to resistance to cancer treatment (1, 8). Several pathways have been described for apoptosis in different systems, but they all converge with activation of the protease caspase 3 and subsequently of endonuclease activity that results in fragmentation of nuclear DNA (4, 9–13). Experimentally, this DNA fragmentation has been demonstrated in model systems as a "ladder" following electrophoretic separation of DNA extracts prepared from the cell population. This method lacks sensitivity because the proportion of apoptotic cells in the population must be large to be detected. A method has been developed to detect DNA damage in single cells called the "comet" or single cell gel electrophoresis assay that can detect effects in subpopulations of cells (14).

The binding of AV by cells undergoing apoptosis has been proposed to be an early event based on correlative studies on cell populations (5): (a) increases in the single AV⁺ cell population occur much earlier than increases in the double-positive cell population; (b) the proportion of AV-binding cells is higher at all times after induction than that of cells with morphological changes in the nucleus; (c) AV binding appeared earlier than cell shrinkage as determined by flow cytometry. Until recently, studies of this type have been correlative by necessity because assays such as AV binding, which require viable cells, and morphological assays could not be performed on the same cell (15). We have developed a method using the ability of the microscope-based LSC to relocate cells that combines the AV-binding assay with assessment of DNA fragmentation by the comet assay in the same cells.

To validate our approach, we selected a well-studied apoptotic system, Jurkat leukemia cells induced to undergo apoptosis by an antibody against Fas. In contrast to other model systems in which drug- or radiation-induced DNA damage initiates the apoptotic program, anti-Fas interacts with a cell surface death receptor to initiate the process. To ensure that we were examining the early events of apoptosis, we have used treatment times of no more than 4 h.

Our initial studies comparing the results obtained by flow cytometry and laser scanning cytometry for PI-AV-FITC-stained cells demonstrated that there was no significant difference between the two methods in the time course of appearance of single- and double-positive cell populations, confirming the results of Bedner *et al.* (11). However, the proportions of AV⁺ cells measured by laser scanning cytometry were higher than those determined by flow cytometry. There are two possible explanations for this difference. The first is that the embedding of the cells in agarose immediately after staining preserves fragile apoptotic cells that may be lost in flow cytometry because of pressure changes through the flow aperture. The second possibility is that the cells might remain intact during flow analysis, but that changes during the apoptotic process in the side scatter parameter used to set regions for flow analysis might remove these cells from the region being analyzed (16). In either case, each positive event detected with the LSC could be confirmed visually as a cell. Another advantage of embedding the cells in agarose is that all of the cells can be examined, avoiding the potential problem associated with

other microscopic assays in which late apoptotic cells may be lost because they cannot attach to glass surfaces (11).

After lysis, electrophoresis, and ethanol fixation, it was possible to reliably relocate nuclei at the sites where cells were first detected for the PI and AV measurements. There was no PI or FITC fluorescence remaining at these locations. When objects were relocated, it was nearly always possible to classify them as intact nuclei, necrotic comets, apoptotic comets, or apoptotic remnants. At the location of single- or double-positive cells, damaged DNA with either an apoptotic or necrotic pattern was evident or small-condensed particles were found. The size of these irregularly shaped particles was ~2–4 μm in diameter, and their color was more yellow than that of normal DNA stained with SYBR Green I. They were also visible on bright field images in contrast to apoptotic or necrotic DNA. These findings suggest that apoptotic remnants are composed of heavily condensed material, probably cross-linked proteins. It has been shown that transglutaminases are activated during the last stages of apoptosis, resulting in cross-linked cellular proteins that prevent disintegration of the apoptotic cells (17).

We did not observe comets with intermediate levels of DNA damage in the double-negative or single-positive populations in these experiments. Most double-negative cells had undamaged DNA with tail moments <10, whereas the single-positive population was composed primarily of heavily damaged cells with apoptotic fragmentation patterns having tail moments >40. In some apoptotic cells, tail moment was not possible to calculate because little or no DNA remained in the head. These observations are in good agreement with field inversion gel electrophoresis data, where an abrupt (within 15 min) DNA fragmentation was found in apoptotic cells (18). We observed intermediate DNA damage (tail moments between 10 and 40) only in the double-positive population, and these cells had comet shapes typical of necrotic DNA damage (19). Thus, it appears that in apoptotic cells, the transition from undamaged DNA to a high degree of DNA fragmentation is very rapid. After the initial fragmentation that gives rise to measurable comets, the DNA is further fragmented, giving rise to comets in which all of the DNA has migrated from the nuclear area during electrophoresis. Finally, there is what appears to be a gradual loss of DNA from the comets leaving only the apoptotic remnants. This last stage may take between 6 and 12 h in Jurkat cells induced by anti-Fas (5).

When measured with the LSC, there was a background of apoptotic cells in the control samples (0 h). These cells that underwent spontaneous apoptosis were all in the late stages of apoptosis. When cells were induced to undergo apoptosis with anti-Fas, the numbers of cells in the early stages increased gradually through the first 3 h and then decreased. This suggests that an initial wave of apoptosis occurs during the first 3 h. Whether or not further waves occur in this population and their relationships to proliferative status of the cells at the time of treatment remain to be determined. Our results confirm that AV binding is an excellent marker for apoptotic cells (5, 20, 21). Virtually all of the cells in the single-positive population had apoptotic comets or apoptotic remnants. In contrast, the double-positive population was composed of cells giving rise to comets having necrotic or apoptotic patterns in about equal numbers. This means that counting only the single-positive cells will underestimate the actual numbers of apoptotic cells.

We have further shown that AV binding does not precede DNA fragmentation because all of the single-positive cells, which are purported to be earlier in the apoptotic process than double-positive cells, have highly fragmented DNA. In contrast to our data, it has been suggested that AV binding is an earlier step in the execution phase than DNA fragmentation (21, 22), based on use of the TUNEL assay to measure DNA fragmentation. This method is not sensitive enough

to detect high molecular size DNA fragmentation that occurs in the early phases of apoptosis, but only detects the final internucleosomal DNA degradation (23, 24). The comet assay, on the other hand, also detects the 50-kb DNA fragments in apoptotic cells (14), so we are detecting the earlier high molecular size fragmentation in our assays using the comet assay. Furthermore, we are looking at early times after the addition of anti-Fas, and if PS exposure was an earlier event than DNA fragmentation, we would expect to find cells containing undamaged DNA in the single- or double-positive populations at these times, which is not the case. Our findings that AV-binding cells have a high degree of DNA fragmentation and loss are also supported by the results of Martin *et al.* (5) showing a correlation between the proportions of peripheral blood neutrophils binding AV after anti-Fas or drug treatment and the numbers of nuclei with sub-G₀/G₁ DNA content as determined by flow cytometry. Our studies with MCF-7 and PC3 demonstrate that the relationship between AV binding and DNA fragmentation is not restricted to cells of hematopoietic origin.

In conclusion, our method using the LSC to relocate cells after subpopulations have been identified and to measure DNA damage by the comet assay provides a powerful tool for studies on apoptosis. This technique can be used to examine other markers of apoptosis, such as binding of mitochondrial specific dyes, to determine their relationship to DNA damage in apoptotic cells. It will also allow analysis of biological relationships between virtually any cell surface or cytoplasmic marker and DNA damage in individual cells.

REFERENCES

1. Lowe, S. W., Schmitt, E. M., Smith, S. W., Osborne, B. A., and Jacks, T. p53 is required for radiation-induced apoptosis in mouse thymocytes. *Nature (Lond.)*, 362: 847-849, 1993.
2. Nagata, S. Apoptosis by death factor. *Cell*, 88: 355-365, 1997.
3. Earnshaw, W. C. Nuclear changes in apoptosis. *Curr. Opin. Cell Biol.*, 7: 337-343, 1995.
4. Khodarev, N. N., Sokolova, I. A., and Vaughan, A. T. Mechanisms of induction of apoptotic DNA fragmentation. *Int. J. Radiat. Biol.*, 73: 455-467, 1998.
5. Martin, S. J., Reutelingsperger, C. P., McGahon, A. J., Rader, J. A., van Schie, R. C., LaFace, D. M., and Green, D. R. Early redistribution of plasma membrane phosphatidylserine is a general feature of apoptosis regardless of the initiating stimulus: inhibition by overexpression of *Bcl-2* and *Abl*. *J. Exp. Med.*, 182: 1545-1556, 1995.
6. Olive, P. L., Banath, J. P., and Durand, R. E. Heterogeneity in radiation-induced DNA damage and repair in tumor and normal cells measured using the "comet" assay. *Radiat. Res.*, 122: 86-94, 1990.
7. Jacks, T., Remington, L., Williams, B. O., Schmitt, E. M., Halachmi, S., Bronson, R. T., and Weinberg, R. A. Tumor spectrum analysis in p53-mutant mice. *Curr. Biol.*, 4: 1-7, 1994.
8. Moos, P. J., and Fitzpatrick, F. A. Taxane-mediated gene induction is independent of microtubule stabilization: induction of transcription regulators and enzymes that modulate inflammation and apoptosis. *Proc. Natl. Acad. Sci. USA*, 95: 3896-3901, 1998.
9. Khodarev, N. N., Sokolova, I. A., and Vaughan, A. T. Association between DNA cleavage during apoptosis and regions of chromatin replication. *J. Cell. Biochem.*, 70: 604-615, 1998.
10. Inohara, N., Koseki, T., Chen, S., Wu, X., and Nunez, G. CIDE, a novel family of cell death activators with homology to the 45 kDa subunit of the DNA fragmentation factor. *EMBO J.*, 17: 2526-2533, 1998.
11. Bedner, E., Li, X., Gorczyca, W., Melamed, M. R., and Darzynkiewicz, Z. Analysis of apoptosis by laser scanning cytometry. *Cytometry*, 35: 181-195, 1999.
12. Liu, X., Zou, H., Slaughter, C., and Wang, X. DFF, a heterodimeric protein that functions downstream of caspase-3 to trigger DNA fragmentation during apoptosis. *Cell*, 89: 175-184, 1997.
13. Tang, D., and Kidd, V. J. Cleavage of DFF-45/ICAD by multiple caspases is essential for its function during apoptosis. *J. Biol. Chem.*, 273: 28549-28552, 1998.
14. Olive, P. L., and Banath, J. P. Sizing highly fragmented DNA in individual apoptotic cells using the comet assay and a DNA cross-linking agent. *Exp. Cell Res.*, 221: 19-26, 1995.
15. Li, X., and Darzynkiewicz, Z. The Schrodinger's cat quandary in cell biology: integration of live cell functional assays with measurements of fixed cells in analysis of apoptosis. *Exp. Cell Res.*, 249: 404-412, 1999.
16. Darzynkiewicz, Z., Juan, G., Li, X., Gorczyca, W., Murakami, T., and Traganos, F. Cytometry in cell necrobiology: analysis of apoptosis and accidental cell death (necrosis). *Cytometry*, 27: 1-20, 1997.
17. Fesus, L. Transglutaminase-catalyzed protein cross-linking in the molecular program of apoptosis and its relationship to neuronal processes. *Cell. Mol. Neurobiol.*, 18: 683-694, 1998.
18. Weis, M., Schlegel, J., Kass, G. E., Holmstrom, T. H., Peters, I., Eriksson, J., Orrenius, S., and Chow, S. C. Cellular events in Fas/APO-1-mediated apoptosis in JURKAT T lymphocytes. *Exp. Cell Res.*, 219: 699-708, 1995.
19. Fairbairn, D. W., Walburger, D. K., Fairbairn, J. J., and O'Neill, K. L. Key morphologic changes and DNA strand breaks in human lymphoid cells: discriminating apoptosis from necrosis. *Scanning*, 18: 407-416, 1996.
20. van Engeland, M., Kuijpers, H. J., Ramaekers, F. C., Reutelingsperger, C. P., and Schutte, B. Plasma membrane alterations and cytoskeletal changes in apoptosis. *Exp. Cell Res.*, 235: 421-430, 1997.
21. van Engeland, M., Nieland, L. J., Ramaekers, F. C., Schutte, B., and Reutelingsperger, C. P. Annexin V-affinity assay: a review on an apoptosis detection system based on phosphatidylserine exposure. *Cytometry*, 31: 1-9, 1998.
22. O'Brien, I. E., Reutelingsperger, C. P., and Holdaway, K. M. Annexin-V and TUNEL use in monitoring the progression of apoptosis in plants. *Cytometry*, 29: 28-33, 1997.
23. Godard, T., Deslandes, E., Lebailly, P., Vigreux, C., Sichel, F., Poul, J. M., and Gauduchon, P. Early detection of staurosporine-induced apoptosis by comet and annexin V assays. *Histochem. Cell Biol.*, 112: 155-161, 1999.
24. Gorczyca, W., Bigman, K., Mittelman, A., Ahmed, T., Gong, J., Melamed, M. R., and Darzynkiewicz, Z. Induction of DNA strand breaks associated with apoptosis during treatment of leukemias. *Leukemia*, 7: 659-670, 1993.

SOP for DNA Isolation

Protocol for the Isolation of Genomic DNA

Involving Sample Preparation and Lysis for the Genomic tip Protocol

This two part protocol is designed for the preparation of up to 20ug of genomic DNA from up to 5×10^6 of cultured or mononuclear blood cells from human blood or bone marrow specimens. The purified genomic DNA ranges from 20 to 150 kb in size.

The cultured cells were grown in cell suspension, and processed according to the methods described in the QIAGEN Genomic DNA Handbook Tissue Culture and Harvesting Protocol (09/97).

Part I: Sample & Reagent Preparation and Lysis Protocol for Cultured Cells

Procedure as follows

Sample Preparation:

Suspension cultures of lymphocyte lines typically contain 2×10^7 cells /ml. 20 G tips will isolate DNA from 5×10^6 cells, so use 0.4 ml per tip max, or an equivalent number of human cells.

Use a 15ml point bottom centrifuge tube – Corning # _____ or Falcon # _____

Isolation of genomic DNA from cell suspension of cultured cells:

- ☐ 1. Centrifuge the appropriate number of cells (5×10^6) for 10 min. @ 1500 $\times g$ (@ 4°C) in a 15 ml centrifuge tube.
- ☐ 2. Discard the supernatant, ensuring all media is completely removed.
- ☐ 3. First Wash cells in 4ml of PBS (same centrifuge conditions)
- ☐ 4. Discard the supernatant, ensuring all media is completely removed.
- ☐ 5. Second Wash cells in 4ml of PBS (same centrifuge conditions)
- ☐ 6. Discard the supernatant, ensuring all media is completely removed.
- ☐ 7. Resuspend in 0.5 ml of PBS (4°C) to a final concentration of $\sim 10^7$ cells/ml.

Reagent Preparation:

- ☐ 1. To obtain maximum purity, and optimal flow rates, it is very important not to use more than 0.5 ml of this suspension.
- ☐ 2. Store or equilibrate Buffer C1 and distilled water in a 50 ml beaker (autoclaved) @ 4°C in refrigerator.

- ☐ 3. Buffers G2, QBT, QC, and QF, are equilibrated to room temperature (Recommend storing at 4 deg C).

{ NB: Buffer C1 and distilled water must be kept on ice during procedure. }

Lysis Protocol for Cultured Cells grown in a Cell Suspension

- ☐ 1. To a 14 ml centrifuge tube add the following:
 - ☐ 1.1 One Part (e.g., 0.5 ml) from the cell suspension of Cultured Cells
 - ☐ 2.2 One Part (0.5 ml) of ice cold C1 buffer
 - ☐ 1.3. Three Parts (1.5 ml) of ice cold distilled water
- ☐ 2. Mix by inverting tube several times until suspension becomes completely translucent. Apparently however, previously frozen samples do not visibly change upon lysis.
- ☐ 3. Incubate on ice for 10 minutes.
- ☐ 4. Centrifuge the lysed cells @ 4°C for 15 minutes at 228 x g = 1000 rpm. Note: 1300 g is recommended in the QIAGEN protocol, which is ~ 2300 rpm. We found this rapid centrifugation may cause the cells to clump and prevent them from complete lysis and protein denaturization. May vary with the type of cells being extracted. If using buffy coats pelleted nuclei is still red after centrifugation, this is due to residual hemoglobin, may need to repeat this step)
- ☐ 5. Discard the Supernant and Add:
 - ☐ 5.1. 0.25ml of ice-cold C1 buffer
 - ☐ 5.2. 0.75ml of ice-cold distilled water to sample.
- ☐ 6. Resuspend the pelleted nuclei by vortexing.
- ☐ 7. Centrifuge 228 x g (1000 rpm) for 10 min., and discard supernatant. (May Freeze Pellets at this point, using cryo-microfuge tube)
- ☐ 8. Start and set the water bath @ 50°C. Use oscillating Blue Water Bath.
- ☐ 9. Add 1ml of G2 buffer and completely resuspend the nuclei for 1min. Resuspend nuclei as thoroughly as possible by vortexing as this step is critical a good flow rate on the Genomic tip.
- ☐ 10. Add 35.7ul of prepared Proteinase K and incubate @ 50°C for ~50 minutes. Note: the QIAGEN protocol uses 25ul; I increased this amount to make the

necessary adjustments per grammage needed Also, the length of incubation depends on how well the nuclei were resuspended in the last step.

Part II: Genomic-tip Protocol

- ☐ 1. Equilibrate a QIAGEN Genomic tip 20/G with 1ml. of QBT buffer and allow to empty by gravity flow.
- ☐ 2. Vortex sample for 10 seconds and add to the equilibrated Genomic tip PROMPTLY.
- ☐ 3. Wash the QIAGEN Genomic tip with 1ml of QC buffer: 3 times.
- ☐ 4. Elute the genomic DNA with 1ml. of QF buffer: 2 times with new collection tubes to collect the eluate.
- ☐ 5. Precipitate the DNA by adding 1.4ml. of isopropanol (@room temp.) To the eluted DNA.
- ☐ 6. Precipitate the DNA by immediately centrifuging @ $\sim 5000 \times g$ (~8500 rpm) for 15 minutes @ 4°C. Carefully remove supernatant.
- ☐ 7. Wash the centrifuged DNA pellet with 1ml. of cold 70% ethanol.
 - ☐ Vortex briefly and centrifuge @ $\sim 5000 \times g$ (~8500 rpm) for 10 minutes @ 4°C.
 - ☐ Carefully remove the supernatant without disturbing the pellet.
 - ☐ Air-dry for 5-10 minutes and resuspend the DNA in 0.1-2ml. of T.E. buffer (pH 8).
- ☐ 8. Dissolve the DNA overnight on a shaker or @ 55°C for 1 - 2 hours.

SOP for DNA Precipitation

PRECIPITATION OF DNA WITH ETHANOL

- 1 Adjust the concentration of the purified DNA, by adding 10M ammonium acetate to make a final solution that contains 2M ammonium acetate. This is done by estimating the volume of the DNA solution that is in TE buffer (pH 8.0). This is necessary to facilitate precipitation of DNA by ethanol.
- 2 Add twice as much of cold 100% ethanol as the entire volume of the sample.
- 3 Mix and store on ice for 10 minutes. (If the DNA is smaller than 1 kb or present at a concentration less than 100 ng/mL, the solution should be stored at -70 degrees Celsius for about 4 hours. For DNA less than 0.2 kb in size, the addition of 0.1 M $MgCl_2$ improves recovery.)
- 4 Centrifuge at 4 degrees Celsius for 10 minutes in a microcentrifuge at top speed (14,000 rpm).
- 5 Discard the supernatant.
- 6 Invert the tubes on a layer of absorbent paper in the hood for an hour, to allow drainage of ethanol. Solvent traces can be removed in a vacuum desiccator or vacuum centrifuge.
- 7 Dissolve the pellet in 25 μ L of HPLC grade water (pH 8.0). Rinse the tube walls with water to ensure dissolution of DNA. Heating to 37 degrees Celsius for at least 5 minutes may help solubilize the DNA as well. Store the DNA solution at 4 degrees Celsius for digestion of DNA.

Conversion of the final solution to 0.2 M

$$C_1V_1 = C_2V_2$$

 C_1 = Conc. Of ammonium acetate V_1 = Volume of ammonium to add C_2 = Conc. Of final solution V_2 = Volume of final solution

Conversion of DNA to make the solution 0.2 M

$$C_1V_1 = C_2V_2$$

 C_1 = 10 mol / 1000 mL V_1 = x mL (x μ L) C_2 = 2 mol / 1000 mL V_2 = (1mL + x mL)

x = ?

 C_1 = 0.01 M V_1 = 0.25 mL C_2 = 0 M V_2 = 1.25 mL

x = 0.25 mL

Reagent	Amount (μ L)
Sample	1000
A. Acetate	250
Ethanol	2500
HPLC H_2O	25

Reagents should be dated with the date they are prepared.

Kit components with the date they were opened.

Dates should be added to experiments.

REAGENTS USED:				
	Date	Lot #	Place of Storage	
dNTP Blend	10/31/01	36227311017	Freezer A	
10X SYBR PCR Buffer	10/31/01	430488911011	Freezer A	
25mM MgCl ₂	10/31/01	430489811018	Freezer A	
AmpliTaq Gold	10/31/01	A02808	Freezer A	
AmpErase UNG	10/31/01	430490311011		
1st set of primers				
NRAS A F	7/19/00			
NRAS B R 2	7/25/00			
2nd set of primers				
NRAS A F	7/19/00			
Step2 1st primer	7/19/00			
100 bp ladder			Freezer A	Gibco
SPECIMENS*:				
	Source	Date Prep.	Place of Storage	System
	Source	Date Prep.	Place of Storage	
1st primer	1 Sample 1	cell	-80 REVCO - C	
	2 Sample 2	cell	-80 REVCO - C	
	3 Sample 3	cell	-80 REVCO - C	
	4 Sample 4	cell	-80 REVCO - C	
	5 Sample 5	cell		
	6 Sample 6	cell		
2nd primer	7 Sample 7	cell	-80 REVCO - C	
	8 Sample 8	cell	-80 REVCO - C	
	9 Sample 9	cell	-80 REVCO - C	
	10 Sample 10	cell		
	11 Sample 11	cell		
	12 100 bp ladder			

NRAS A and NRAS B 2 & NRAS A and Step2 1st primer
of reactions

	Vol. Total	Components	volume per reaction
7	Mix		
Check			
Off	ul	MIX 1	25
		17.5 ul 10X SYBR PCR buffer - PE	2.5
		17.5 ul 25 mM MgCl ₂ - PE	2.5
		14 dNTP Blend	2
		1.75 NRAS A F	0.25
		1.75 NRAS B R 2	0.25
		0.875 Amplitaq Gold polymerase From PE	0.125
		1.75 AmpErase UNG	0.25
		105.88 water	15.125
Sum	161	Volume Mix Per Tube ul	23
		Check on vol total mix	161

	Vol. Total	Components	volume per reaction
6	Mix		
Check			
Off	ul	MIX 2	25
		15 ul 10X SYBR PCR buffer - PE	2.5
		15 ul 25 mM MgCl ₂ - PE	2.5
		12 dNTP Blend	2
		1.5 NRAS A F	0.25
		1.5 Step2 1st primer	0.25
		0.75 Amplitaq Gold polymerase From PE	0.125
		1.5 AmpErase UNG	0.25
		90.75 water	15.125
Sum	138	Volume Mix Per Tube ul	23
		Check on vol total mix	138

Suggest: Add water first, then PCR mix, then sample.

Tube Number	Specimen	sample vol ul	Vol PCR Mix ul	Total Vol Calc	Total Vol Planned
1	Sample 1	2 MIX 1	23	25	25
2	Sample 2	2 MIX 1	23	25	25
3	Sample 3	2 MIX 1	23	25	25
4	Sample 4	2 MIX 1	23	25	25
5	Sample 5	2 MIX 1	23	25	25
6	Sample 6	2 MIX 1	23	25	25
7	Sample 7	2 MIX 2	23	25	25
8	Sample 8	2 MIX 2	23	25	25
9	Sample 9	2 MIX 2	23	25	25
10	Sample 10	2 MIX 2	23	25	25
11	Sample 11	2 MIX 2	23	25	25
12	100 bp ladder				

Running EZ-Gel

Label GeneAmp tubes to match samples

Use Sigma Gel Loading Solution

Carefully press start once for 2 min prerun; Then load specimens, then press a second time for Run. Time Run

	Tube	DEPC H2O ul	Loading Soln	Sample ul	
Sample 1	1	16	0	4	Place in a 65 deg C MJ unit for 10 min and place immediately on ice.
Sample 2	2	16	0	4	
Sample 3	3	16	0	4	
Sample 4	4	16	0	4	
Sample 5	5	16	0	4	
Sample 6	6	16	0	4	
Sample 7	7	16	0	4	SAVE TUBE 12 in FREEZER
Sample 8	8	16	0	4	
Sample 9	9	16	0	4	
Sample 10	10	16	0	4	
Sample 11	11	16	0	4	PLACE IN A WATERBATH FOR 5 MIN (37°C) and put immediately on ice
100 bp ladder	CONTROL	19	0	1	

Time Started:

Time Stopped:

NRAS A and NRAS B PCR Mix using Taq polymerase

Sample	temp. vol	abbrev. Id.	sample type	extr. on	results
1	2	Sample 1	cell		
2	2	Sample 2	cell		
3	2	Sample 3	cell		
4	2	Sample 4	cell		
5	2	Sample 5	cell		
6	2	Sample 6	cell		
7	2	Sample 7	cell		
8	2	Sample 8	cell		
9	2	Sample 9	cell		
10	2	Sample 10	cell		
11	2	Sample 11	cell		
12	2	100 bp ladder			

Cells:

Date of Preparation:

Recovery Standard:

Salmon Testes DNA in 0.1 M Tris Buffer pH 7.2

2/2/00

- See setup for DNA digestion experiments

10 M Ammonium Acetate Buffer

ammonium acetate ($\text{NH}_4\text{COOCH}_3$)

MW = 77.08 g/mol

Molarity (mol/L)	MW (g/mol)	Amt (g/L)
10	77.08	770.8

Modifications to only make 500 mL of buffer instead of 1L

Amt (g/L)	Conversion factor (L/mL)	New amt (g/L)
770.8	0.5/500	384.4

CELL COUNTS

Cell count is determined by Trypan blue exclusion by the following:

62.5 ul Trypan blue

37.5 ul Hank's balanced salt solution

25 ul cell suspension

mix and let stand for 5 min. and count on a hemocytometer

take avg. per square multiplied by 5×10^4

cell count = 180,000

The following chart will make the calculations. Enter the values for each square counted.

sample	A		B		C	
	square	live	dead	live	dead	live
1	4	0	5	1	0	0
2	0	0	1	0	0	0
3	5	1	1	0	0	0
4	0	0	2	0	0	0
5	3	1	0	0	0	0
6	5	0	2	0	0	0
7	2	1	2	0	0	5
8	3	0	4	1	0	0
9	7	0	1	0	0	0
10	8	1	3	0	0	0
total	37	4	21	2	0	0
divide by 10	3.7	0.4	2.1	0.2	0	0
multiply by 5	18.5	2	10.5	1	0	0
e104	185000	20000	105000	10000	0	0
Total Cells		205000		115000		0
Viability		90.2439		91.30435	#DIV/0!	#REF!

Note the changes in the volume of the cell suspension and the medium.

By changing the number of slides in the formula on this sheet, the program will automatically adjust the volumes.

This sheet was taken from this file: C:\ann's comets\supplies2.xls May be a later version of the files.

BCNU WEIGHING PROCEDURES

The following is a procedure for determining Treatment dosage

1. Weigh microtubes (Sarstedt 1.5 ml. microtube)
2. Adjust coarse adjustment weight using "1/2"
3. Fine tune on "1" (bars between teeth)
4. Remove static (when necessary) using static gun
5. Take microtubes to chemical exhaust hood
6. Using a spatula take and add small amount to respective tube
7. Close tube and weigh on Mettler; weigh on "1"
8. Calculate the number of Moles in the tube

Using Mettler H54AR

begin weight of tube = 1.548 g
 end weight of tube w/BCNU = 1.5598 g
 weight of BCNU = 11.8 mg

To make a 1 M Standard, use formula: weight in g/Molecular Weight = ml solvent needed for 1M

Weighing
 amt of (mg) = 11.8

Date of preparation: 2-9-00

Compound	MW (g/mol)	Amt (mg)	1/MW (mol/g)	1/Molarity (uL/mol)	Amt (uL)	Stock Label
BCNU	214.1	11.8	0.004670715	10000000	551.144325 = 100 mM	BCNU 100mM

Dilutions

Stock Label	Stock mM	Stock ul	Solvent	Solvent ul	New Conc (mM)	New Label	100 Fold Dil Gives uM
BCNU 100mM	100	100	ethanol	900	10	BCNU 10mM	100

The stds were frozen and placed in the -80 freezer

BCNU Dose Response Assay Experiment For DNA And Cultured Lymphocytes Cells

Cells	BCNU Conc (mM)	Tube #	mL cells	mL RPMI	mL DNA*	mL Tris	Rx (10ul)	Vol Check (mL)	Exposure	/ Label	Ammonium Acetate (uL)	Ethanol (uL)
	0	1	0.666	0.324			ETHANOL	1	2 hours		NA	NA
	10	2	0.666	0.324			BCNU 100mM	1	2 hours		NA	NA
	100	3	0.666	0.324			BCNU 10mM	1	2 hours		NA	NA
	0	4			0.01	0.98	ETHANOL	1	2 hours			
	10	5			0.01	0.98	BCNU 100mM	1	2 hours			
	100	6			0.01	0.98	BCNU 10mM	1	2 hours			

**Cells were processed by: SOP for DNA Isolation. This can be found at

C:\Anne\DNA Adducts\Singer Bodell Method\SOP1

DRUG CALC

Calculations for treatment solution: an example with Carmustine

Treatment Molarity Values: 10, 50, 100, 500, 1000 μ M

Mix one ml of the highest concentration treatment and dilute it down to provide the other concentrations.

Treatment Molarity	Molarity of stock	moles/liter X grams/mole equals mg/liter		
		moles/liter	grams/mole	equal mg/L
100 μ M	10000 μ M	0.01	214.1	2.14

C:\annel\DNA Adducts\ SOP FOR Cell Exposure Assays2

TREATMENT OF CELLS WITH CARMUSTINE

Molecular formula of Carmustine: $C_5H_9Cl_2N_3O_2$

Carmustine solution - a powder; mw = 214.1 g/mol
 $(214.1 \text{ g} \times 1 \text{ mole} \times 100 \mu\text{mole}) / (1 \text{ mole} \times 100,000 \mu\text{mole} \times 1000 \text{ mL})$
 $= 0.0002141 \text{ g/ mL DMSO}$

This is a very small amount to weigh out (in fact impossible). Therefore, first weigh out a very small amount of drug and then next calculate its molarity.

amt of Carmustine (g) =	0.01
-------------------------	------

Compound	MW (g/mol)	Amt (g)	1/MW (mol/g)	1/Molarity (uL/mol)	Amt (uL)	
BCNU	214.1	0.01	0.00467071	10000000	467.0715	= 100 mM

Notes on Singer and Bodel Nature Paper 1978

Digested 100ul = 1 mg DNA in Sterile Water

In Nature Paper:	ul
DNA @10mg/ml	100
0.5 M Tris 7.3 buffer	20
1 M MgCl ₂	2
DNA Ase	20
SVP	20
Bact. Alk Phos	8
Acid Phosphatase	8

DNAase I is 5 mg/ml, 2465 Units per mg, 12325 U/ml

SVP is 5 mg/ml, 32 Units per mg, 160U/ml

Alkaline Phos 5 mg/ml, 37 Units/mg, 185 U/ml

Acid Phosp 5 mg/ml, 16 U/mg, 80 units/ml

Worthington Biochemical Support recommended reconstituting enzymes with buffer and freezing at -20 or -80 C in small aliquots.
Could reconstitute with water, but may get unstable pH that lowers activity.

USING 2/1/00 Working Stocks:

ul	300 (Buffer was used to prep DNA)
	0
	0
	80 Ours is 1/4 strength, use 4x
	20
	4 Ours is 2x units/ml, use 1/2
	8

notes (cont.)

Working procedure for preparing master stocks according to Nat.

	Enzyme	Tris		
	(mg)	Buffer* (ml)	mg/ml	U/ml
DNAase I 1400 U/mg Powder 25 mg	25	2.5	10	14000
SVP 20 units per mg dry wt, have 100 units=5mg	5	0.666	7.5	150
Alk Phos 39.9 units/mg protein, have 1 mg, 9.1 mg/ml, have 109ul, 360 u/	1	0.2	5	150
Acid Phosphatase 15 U/mg, have 1 g	5	1		75

Working procedure used for preparing Master Stocks (some made before paper was located)

	Enzyme	Tris			
	Label	(mg)	Buffer* (ml)	mg/ml	U/ml Buffer
DNA	STDNA1	2.9	3.48	0.83	Not sterile, with MgCl ₂
DNAase I 1400 U/mg Powder 25 mg	DP1	2.6	1.04	2.5	Not sterile, with MgCl ₂
SVP 20 units per mg dry wt, have 100 units=5mg	VPH1	5	0.737	6.78	Sterile, no MgCl ₂
Alk Phos 39.9 u/mg prot, have 1 mg, 9.1 mg/ml, have 109ul, 360 u/ml	BAPF1	1	0.2	5	Sterile, no MgCl ₂
Acid Phosphatase 15 U/mg, have 1 g	AP1	5	1	5	Sterile, no MgCl ₂
Our other prep. Of Alkaline Phosphatase 35.9 u/mg P, 20.3 mgP/ml = 700 U/ml 5 mg got 0.246 ml					

PREPARATION OF 0.1M TRIS BUFFER

Tris:

(Tris[hydroxymethyl]amino-methane)

 $C_4H_{11}NO_3$

MW (g/mol) = 121.1

Weight = MW * Molarity

MW (g/mol)	Molarity (mol/L)	Cal Weight (g)	Act. Weight (g)
121.1	0.1	6.055	6.0503

*Only 500 mL of buffer was made, so the weight was adjusted.

To Prepare 1 liter 0.1M Tris Buffer

- 1 For a 1L solution weigh out 12.11 g of Tris
- 2 Place the weighed out Tris into a 1L bottle and add 1 L of sterile water*
- 3 Check the pH of the solution by using the pH meter to make sure it is at approx. 7.2
- 4 If the pH is too high add HCl until it is stabilized at 7.2
- 5 If the pH is too low add NaOH until it is stabilized at 7.2
- 6 Following the preparation of the buffer it is stored in the refrigerator.

*Water can be sterilized by putting it through a syringe filter or a more developed system.

Actual pH = 7.2

Notes:

The buffer preparation of 2-3-00 was made with sterile water. No $MgCl_2$ was used to prepare this buffer.

Also in future experiments we might like to use 0.1M buffer for the resuspension of the DNA and 0.5M buffer for the digestion reaction. A separate buffer containing 1M $MgCl_2$ will also be made for future experiments.

Add 95.21 mg to 100 ml of the 0.1M Tris Buffer

Original Set-up of stock solutions. Only DNA and Dnase was set-up in this manner.

HPLC INJECTION LOOP HOLDS 200ul. Will set up for 500 ul digestion mixes to allow for losses in filtration and replicate injections:

	DNA	DNA-ase	SVP	Alk P
Weight (ug)	250	250	100	100
Vol (ul)	300	100	50	50

	Stock	Buffer	Vol of Stock Soln	Actual	Actual
	ug		ug	ug	ml
DNA	250	300	2500	3	2900
DNase	250	100	2500	1	2600
SVP	100	50	1000	500	2
Alk P	100	50	1000	500	2
					0
					0

Notes: Original Set-up of stock solutions. Only DNA and Dnase was set-up in this manner. The following reagents were prepared in a separate manner described in Stock2.

PREPARATION OF STOCK REAGENTS FOR DIGESTION RXN

Date: 2-3-00

Specimen	Abbr.*	Label	Amt Enzyme (mg)	Tris Buffer (mL)	Conc (mg/mL)	U/mL	0.1M Tris Buffer** pH=7.2
Salmon Testes DNA	no	STDNA1	2.9	3.48	0.83		Not sterile, with MgCl ₂
Deoxyribonucle ase	DP	DP1	2.6	1.04	2.5	3500	Not sterile, with MgCl ₂
Snake venom phosphodiester ase	VPH	VPH1	5	0.67	7.50	150	Sterile, with MgCl ₂
Bacterial Alkaline phosphatase***	BAPF	BAPF1	1	0.2	5	150	Sterile, with MgCl ₂
Wheat germ (acid) phosphatase	AP	AP1	5	1	5	75	Sterile, with MgCl ₂

*Abbreviations are from Worthington Biochemicals labeling system.

**Tris Buffer used for DNA and DNase was 0.1 M Tris and 0.01 MgCl₂. The remaining three enzymes were prepared in 0.1M Tris Buffer with sterile water and without MgCl₂.

***BAPF was not put into buffer, bc it is already in solution and its concentration was correct. The amount needed was taken directly from the original vial.

Notes:

Each reagent (except BAPF) was pipetted into individual aliquots and stored in the -80 freezer. This was done to prevent the loss of activity by the thawing/refreezing process and also recommended by the technical support of Worthington. A box (it is labeled DNA ADDUCT ASSAY DNA DIGESTION) containing all the reagents (except BAPF1) is in the -80 freezer, second shelf from the bottom. BAPF is stored in refrigerator A. There is enough enzymes to perform 8 separate digestions. There is an excess of both VPH1 and AP1 and these enzymes are stored in the -80 freezer.

DNA DIGESTION MIX

2/3/00

Components	Volume (uL)
STDNA1	300
0.1M Tris Buffer w MgCl ₂	
DP1	80
VP1	20
BABF1	4
AP1**	8

*already mixed with enzymes

**not mixed with buffer

Components	Volume (uL)
DNA digested 2-1-00	100
0.1M Tris Buffer w MgCl ₂	
DP1	80
VP1	20
BABF1	4
AP1**	8

*already mixed with enzymes

**not mixed with buffer

Digestion Mix for Future Experiments:

of Samples = 8

Components	Volume (uL)
Specimen	
0.5M Tris Buffer	800
1M MgCl ₂	16
DP1	640
VP1	160
BABF1	32
AP1	64
total	1712

Following the set up the tubes were put in the incubator/shaker at 37 degrees for 24 hours.

In the future will mix DP1 up 4x as concentrated - use 20 ul

0.1 M Tris Buffer, containing MgCl₂ was used for this digestion.

INACTIVATION & PURIFICATION

Following the digestion the mixture is:

1. Heated at 100 degrees for 90s
2. Passed through a centrifugal filter with a pore size of 0.2 μm

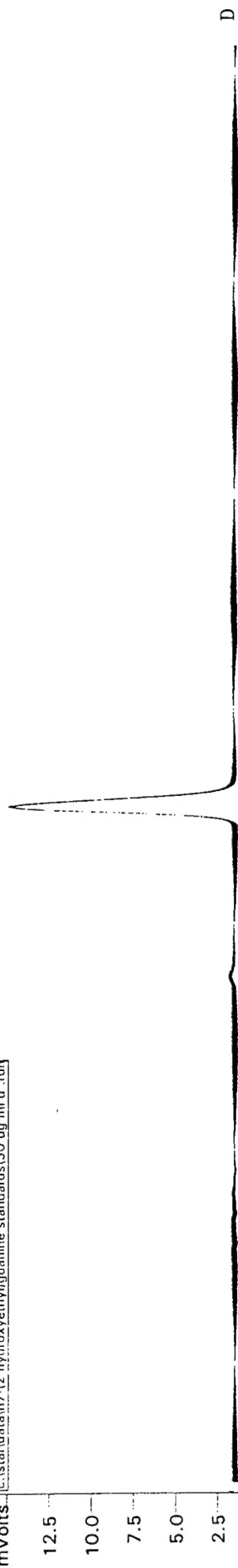
FILTRATION

Filter Hydrolysate with 0.2 μm centrifugal microfilters at 1300 g for 5 min

The following two figures illustrate HPLC analysis of DNA adducts for N7-(2 hydroxyethyl)guanine (N7-HOEtG) standards. Sodium acetate buffer at pH 5.4 was used as mobile phase A and methanol was used as mobile phase B. The N7-HOEtG standards were run with the following HPLC isocratic program: 90% A and 10%B for 12 min. N7-HOEtG in 15 ul mobile phase was injected at concentrations of 2 ug/ml (A), 5 ug/ml (B), 10 ug/ml (C), 50 ug/ml (D).

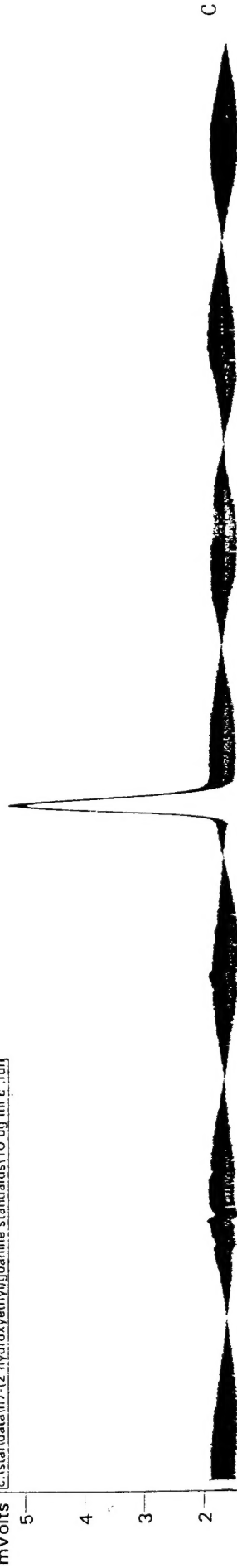
mVolts

c:\star\data\n7-12 hydroxyethylguanine standards\50 ug ml d .run



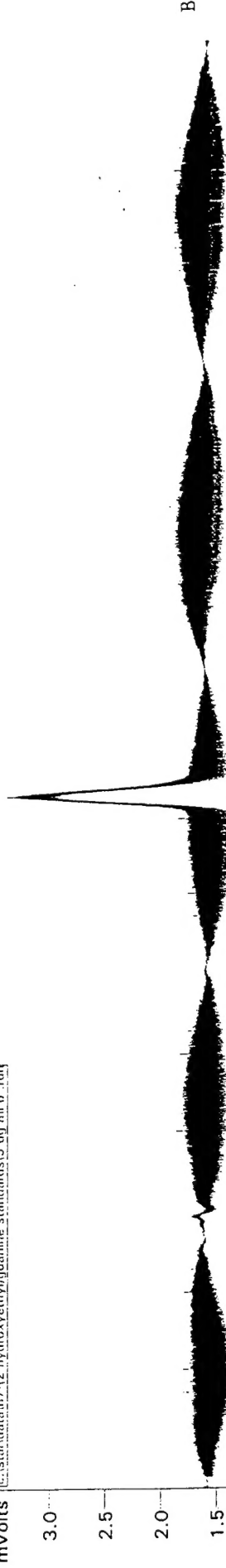
mVolts

c:\star\data\n7-12 hydroxyethylguanine standards\10 ug ml c .run



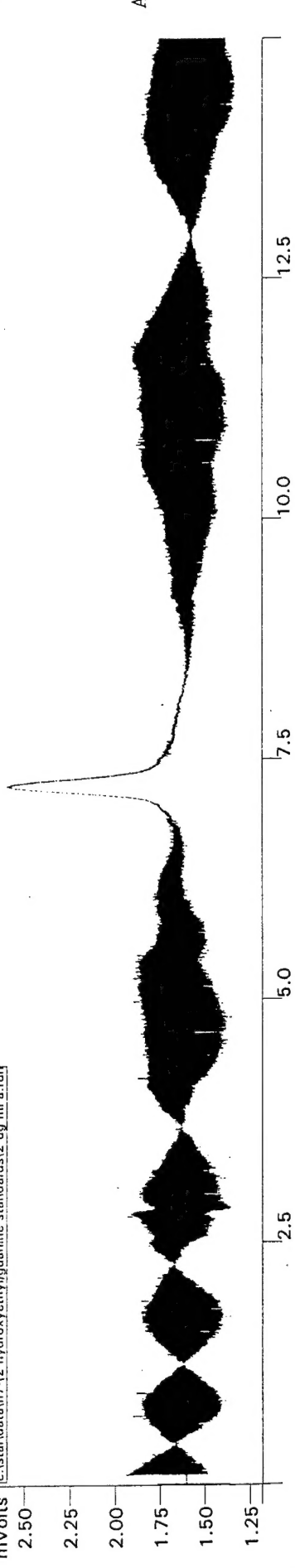
mVolts

c:\star\data\n7-12 hydroxyethylguanine standards\5 ug ml b .run



mVolts

c:\star\data\n7-12 hydroxyethylguanine standards\2 ug ml a .run



Minutes

c:\star\data\7-12 hydroxyethylguanine standards\2 ug ml a.run
c:\star\data\7-12 hydroxyethylguanine standards\5 ug ml b.run
c:\star\data\7-12 hydroxyethylguanine standards\10 ug ml c.run
c:\star\data\7-12 hydroxyethylguanine standards\50 ug ml d.run

mVolts

17.5

15.0

12.5

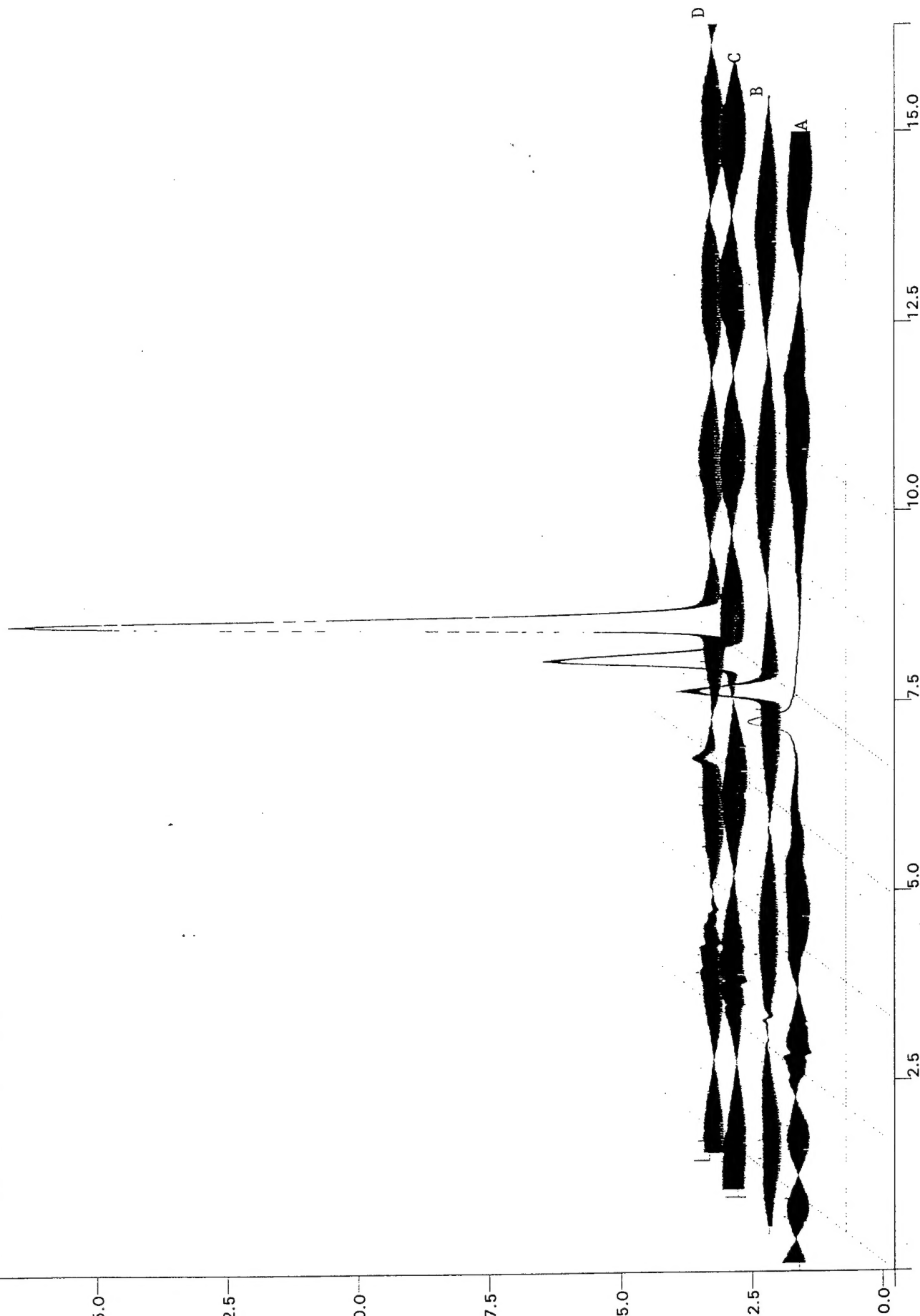
10.0

7.5

5.0

2.5

0.0



Minutes